Timing and climate forcing of volcanic eruptions for the past 2,500 years

M. Sigl[1*], M. Winstrup[2], J.R. McConnell[1], K.C. Welten[3], G. Plunkett[4], F. Ludlow[5], U. Büntgen[6], M. Caffee[7,8], N. Chellman[1], D. Dahl-Jensen[9], H. Fischer[10], S. Kipfstuhl[11], C. Kostick[12], O.J. Maselli[1], F. Mekhaldi[13], R. Mulvaney[14], R. Muscheler[13], D.R. Pasteris[1], J.R. Pilcher[4], M. Salzer[15], S. Schüpbach[10], J.P. Steffensen[9], B.M. Vinther[9], T.E. Woodruff[7]

[1] Desert Research Institute, Nevada System of Higher Education, Reno, NV 89512, USA

[2] Department of Earth and Space Sciences, University of Washington, Seattle, WA 98195, USA

[3] Space Sciences Laboratory, University of California, Berkeley, CA 94720, USA

[4] School of Geography, Archaeology & Palaeoecology, Queen's University Belfast, Belfast BT7 1NN, UK

[5] Yale Climate & Energy Institute, and Department of History, New Haven, CT 06511, USA

[6] Swiss Federal Research Institute WSL, 8903 Birmensdorf, Switzerland

[7] Department of Physics, Purdue University, West Lafayette, IN 47907, USA

[8] Department of Earth, Atmospheric, and Planetary Sciences, Purdue University, West Lafayette, IN 47907, USA

[9] Centre for Ice and Climate, Niels Bohr Institute, University of Copenhagen, 2100 Copenhagen, Denmark

[10] Climate and Environmental Physics, and Oeschger Centre for Climate Change Research, University of Bern, 3012 Bern, Switzerland

[11] Alfred-Wegener-Institut Helmholtz-Zentrum für Polar- und Meeresforschung, 27570 Bremerhaven, Germany

[12] Department of History, The University of Nottingham, Nottingham NG7 2RD, UK

[13] Department of Geology, Quaternary Sciences, Lund University, 22362 Lund, Sweden

[14] British Antarctic Survey, Natural Environment Research Council, Cambridge, CB3 0ET, UK

[15] The Laboratory of Tree-Ring Research, University of Arizona, Tucson, AZ 85721, USA

Volcanic eruptions contribute to climate variability, but quantifying these contributions has been limited by inconsistencies in the timing of atmospheric volcanic aerosol loading determined from ice cores and subsequent cooling from climate proxies such as tree rings. Using new records of atmospheric aerosol loading developed from high-resolution, multi-parameter measurements from an array of Greenland and Antarctic ice cores as well as distinctive time markers to constrain chronologies, here we resolve these inconsistencies and demonstrate that large eruptions in the tropics and high latitudes were primary drivers of Northern Hemisphere interannual-to-decadal temperature variability during the past 2,500 years. Overall, cooling was proportional to the magnitude of volcanic forcing and persisted for up to ten years after some of the largest eruptive episodes. Our revised timescale now firmly implicates volcanic eruptions as catalysts in the major 6th century pandemics, famines, and socioeconomic disruptions in Eurasia and Mesoamerica while allowing multi-millennium quantification of climate response to volcanic forcing.

Volcanic eruptions are primary drivers of natural climate variability – as sulfate aerosol injections into the stratosphere shield the Earth's surface from incoming solar radiation, leading to short-term cooling at regional-to-global scales[1]. Temperatures during the past 2,000 years have been reconstructed at regional[2], continental[3], and global scales[4] using proxy information from natural archives. Tree-ring-based proxies provide the vast majority of climate records from mid- to high-latitude regions of predominantly the Northern Hemisphere (NH), whereas ice-core records (e.g., $\delta^{18}O$) represent both polar regions[3]. Climate forcing reconstructions for the Common Era (CE) – including solar (e.g., ^{10}Be)[5] and volcanic (e.g., sulfate)[6,7] activity – mostly derive from ice-core proxies. Any attempt to attribute reconstructed climate variability to external volcanic forcing – and distinguish between response, feedback, and internal variability of the climate system – requires ice-core chronologies that are synchronous with those of other climate reconstructions. In addition, multi-proxy climate reconstructions[2-4] derived from ice cores and other proxies such as tree rings will

have diminished high-to-mid-frequency amplitudes if the individual climate records are on different timescales. Magnitudes and relative timing of simulated NH temperature response to large volcanic eruptions are in disagreement with reconstructed temperatures obtained from tree rings[8,9], but it is unclear to what extent this model/data mismatch is caused by limitations in temperature reconstructions, volcanic reconstructions, or implementation of aerosol forcing in climate models[9-11]. The hypothesis of chronological errors in tree-ring-based temperature reconstructions[8,9] offered to explain this model/data mismatch has been tested and widely rejected[11-14], while new ice-core records have become available providing different eruption ages[15,16] and more precise estimates of atmospheric aerosol mass loading[17] than previous volcanic reconstructions. Using documented[18] and new ice-core-based eruption ages[16], strong summer cooling following large volcanic eruptions has been recorded in tree-ring-based temperature reconstructions during the 2nd millennium CE with a one-to-two year lag similar to that observed in instrumental records after the 1991 Pinatubo eruption[19]. An apparent seven-year delayed cooling observed in individual tree-ring series relative to Greenland ice-core acidity peaks during the 1st millennium CE, however, suggests a bias in existing ice-core chronologies[20,21]. Using published ice-core chronologies, we also observed a seven-year offset between the timing of sulfate deposition in North Greenland and the start of tree-ring growth reduction in a composite record of five multi-centennial tree-ring summer temperature reconstructions ("N-Tree") from the NH between 1 and 1000 CE (Methods), whereas tree-ring response was effectively immediate for eruptions occurring after 1250 CE (Fig. 1).

A precise time marker across hemispheres and climate proxies. Independent age markers to test the accuracy of tree-ring and ice-core chronologies recently have become available with the detection of abrupt enrichment events in the ^{14}C content of tree rings. Rapid increases of atmospheric ^{14}C were first identified in individual growth increments of cedars from Japan between 774 and 775 CE[22] and between 993 and 994 CE[23]. The presence and timing of the event in 775 CE (henceforth, 775 event) has been reproduced by all measurements performed on tree rings at annual (or higher) resolution – including tree cores from Germany[24], the Alps[12], the Great Basin[25]

(USA), and Siberia[25]. Recent identification of the same 775 CE event in kauri wood samples from New Zealand in the Southern Hemisphere (SH) demonstrates the global extent of the rapid 14C increase and provides further constraints on the event's exact timing (March 775 ± 6 months) due to the asynchronous SH growing season[26]. While the cause of the 775 and 994 events is still debated[22,24,27], they might produce an excess of cosmogenic ^{10}Be through the interaction of high-energy particles with atmospheric constituents[28,29]. Since both of these radionuclides are incorporated rapidly into proxy archives via aerosol deposition (^{10}Be in ice cores) and photosynthesis ($^{14}CO_2$ in tree rings), isotopic anomalies caused by these extraterrestrial events provide a global time marker to directly link ice-core records to tree-ring chronologies[27]. The latter serve as an absolute and precise time marker[31], verified (at least since 775 CE) by the coherence of the rapid increase in ^{14}C in all tree-rings records for which high-resolution analyses were performed, including those speculated to be at risk of missing rings[8]. We measured ^{10}Be concentrations at approximately annual resolution in four ice cores – NEEM-2011-S1, TUNU2013, and NGRIP in Greenland, and the West Antarctic Ice Sheet Divide Core (WDC) – over depth ranges encompassing the year 775 as dated in existing ice-core chronologies in order to provide a direct, physically-based test of any dating bias in these chronologies (Fig. 1, Extended Data Fig. 1, Methods). Both polar ice sheets contain ^{10}Be concentrations exceeding the natural background concentration (>150%; 6σ) for one-to-two consecutive years, compatible with the 775 CE event observed in tree rings. Using the original ice-core age models[16,30], the ages of the ^{10}Be maxima in NEEM-2011-S1, NGRIP, and WDC are 768 CE, offset by 7 years from the tree-ring event. A further ^{10}Be anomaly measured in NEEM-2011-S1 at 987 CE, compatible with the 994 CE event in tree rings, suggests a chronological offset was present by the end of the first millennium CE (Fig. 1). Several different causes may have contributed to the offset (Methods).

Revised ice-core chronologies. Given the detection of a bias in existing ice-core chronologies, we developed new timescales prior to the 1257 Samalas eruption[31] using highly resolved, multi-parameter aerosol concentration records from three ice cores: NEEM-2011-S1, NEEM, and WDC. We

used the StratiCounter program, an automated, objective, annual-layer detection method based on Hidden Markov Model (HMM) algorithms[32] (Methods). For NEEM-2011-S1, obtained confidence intervals for the layer counts allowed us to improve the dating further by constraining the timescale using the 775 CE ^{10}Be anomaly and three precisely dated observations of post-volcanic aerosol loading of the atmosphere (Fig. 2, Extended Data Tables 1-3, Methods, Supplementary Data). We evaluated the accuracy of our new chronologies ("WD2014" for WDC and "NS1-2011" for NEEM) by comparison to (1) an extensive database of historical volcanic dust veil observations (Extended Data Fig. 2, Methods, Supplementary Data), (2) ice-core tephra evidence (Methods), and (3) the 994 CE event (Methods, Fig. 2). Using the new timescales, we found large sulfate signals in Greenland (e.g. 681, 574, 540 CE) between 500 and 2000 CE that frequently occurred within ±1 year from comparable – and independently dated – signals in Antarctica. These bipolar signals can now be confidently attributed to large tropical eruptions (Fig. 2). Back to 400 BCE, other large sulfate peaks (e.g., 44 BCE) were synchronous to within ±3 years (Fig. 2). We conclude that the revised ice-core timescales are accurate to within less than ±5 years during the past 2,500 years based on combined evidence from radionuclides, tree rings, tephra analyses, and historical accounts. Compared to the previous chronologies, age models differ prior to 1250 CE by up to 11 years (GICC05, Greenland) and 14 years (WDC06A-7, Antarctica) (Extended Data Fig. 3).

Reconstruction of volcanic aerosol forcing for the past 2,500 years. Employing our revised timescales and new high-resolution, ice-core sulfur measurements, we developed an extended reconstruction of volcanic aerosol deposition since early Roman times for both polar ice sheets from which we then estimated radiative forcing using accepted transfer functions[15] (Fig. 3, Methods). This forcing series is characterized by improved dating accuracy, annual resolution, and a larger number of ice-core records in the Antarctic ice-core sulfate composite[17] than previous reconstructions[6,7]. It spans 2,500 years, allowing investigation of climate-volcano linkages more accurately and earlier than with previous reconstructions. It also provides perspective on volcanic influences during major historical epochs, such as the growth of Roman imperial power and subsequent decline of the

migration period in Europe – times of (1) demographic and economic expansion as well as relative societal stability and (2) political turmoil and population instability, respectively[33]. With improved dating and lower volcanic-sulfate detection limits from the Antarctic array[17], we were able to detect, estimate, and attribute volcanic aerosol loading and forcing from 283 individual eruptive events during this period (Fig. 3). We attributed about 50% to mid-to-high latitudes NH sources, while 81 were attributed to tropical eruptions (having synchronous sulfate deposition on both polar ice sheets). These tropical volcanic eruptions contributed 64% of total volcanic forcing throughout the period, with five events exceeding the sulfate loading from Tambora, 1815 (Fig. 3, Extended Data Table 4). Events in 426 BCE and 44 BCE rival the great 1257 CE Samalas eruption (Indonesia) as the largest sulfate producing eruptions during this time. These two earlier events have not been widely regarded as large tropical eruptions with potential for strong climate impact[20], due to the lack of complete and synchronized sulfate records from Greenland and Antarctica. We base the claim that these two eruptions were tropical in origin and caused significant radiative perturbations on the observation that ice cores from Greenland and Antarctica record coeval and exceptionally high volcanic sulfate concentrations (within their respective uncertainties). Both these events were followed by strong and persistent growth reduction in tree-ring records[34] (Fig. 2) typically observed after large tropical eruptions during the Common Era (Fig. 3).

Climate impact from large volcanic eruptions. Superposed epoch analyses (Methods) performed on the "N-Tree" composite record centered on the largest volcanic signals between 500 BCE and 1250 CE as well as between 1250 and 2000 CE, show a clear post-volcanic cooling signal. For both periods, maximum tree-ring response lagged the date of initial increase of sulfate deposition by one year (Fig. 2), consistent with the response observed if using only historically documented eruptions with secure dating for the past 800 years[18]. The sharp and immediate (i.e., ≤1 year lag) response of tree growth to the ice-core volcanic signal throughout the past 2,500 years further corroborates the accuracy of our new ice-core timescales (Extended Data Fig. 4). Of the 16 most negative tree-growth anomalies (i.e., coldest summers) between 500 BCE and 1000 CE, 15 followed large volcanic signals –

154 with the four coldest (43 BCE, 536, 543, and 627 CE) occurring shortly after several of the largest
155 events (Extended Data Tables 4, 5). Similarly, the coldest summers in Europe during the Common
156 Era[3] were associated with large volcanic eruptions (Extended Data Table 5). Reduced tree growth
157 after volcanic eruptions also was prominent in decadal averages of the "N-Tree" composite. All 16
158 decades with the most reduced tree growth for our 2,500-year period followed large eruptions (Fig.
159 3, Extended Data Table 5). In many cases, such as the coldest decade from 536 to 545 CE[3], sustained
160 cooling was associated with the combined effect of several successive volcanic eruptions.

161 Strong post-volcanic cooling was not restricted to tropical eruptions; it also followed NH
162 eruptions (Fig. 4), with maximum cooling in the year of volcanic-sulfate deposition. In contrast to the
163 average of the 19 largest CE tropical eruptions, however, the NH-only eruptions did not give rise to
164 any significant long-term cooling effect (Fig. 4). Persistence of implied post-volcanic cooling following
165 the largest tropical eruptions is strongly expressed in temperature reconstructions based on tree-
166 ring width measurements (e.g., Alps), with recovery times of more than 10 years. Persistent cooling,
167 with temperature reduction significantly below the pre-eruption baseline for six consecutive years,
168 also is observed in temperature reconstructions based on maximum latewood density (e.g.,
169 Northern Scandinavia), the preferred proxy to quantify volcanic cooling contributions on climate due
170 to less marked biological memory effects[35] (Fig. 4). These findings indicate that eruption-induced
171 climate anomalies following large tropical eruptions may last longer than is indicated in many
172 climate simulations (<3–5 years)[9,36,37] and that potential positive feedbacks initiated after large
173 tropical eruptions (e.g., sea-ice feedbacks) may not be adequately represented in climate
174 simulations[38,39]. The five-year averaged (lag 0 to lag 4 years) cooling response over three NH regions
175 (Methods) following the 19 largest CE tropical eruptions was -0.6 ± 0.2 °C (2 standard error of the
176 mean (SEM)), that of large NH eruptions was -0.4 ± 0.4 °C with strongest cooling induced in the high
177 latitudes. Overall, cooling was proportional to the magnitude of volcanic forcing, with stratospheric
178 sulfate loading exceeding that of Tambora inducing the strongest response of -1.1 ± 0.6 °C (Figs. 3,

4). We believe the values represent lower estimates of the actual cooling as the timing of ice-core-derived forcing and tree-ring indicated cooling have not been synchronized for the volcanic events.

Global climate anomalies in 536-550 CE. Our new dating allowed us to clarify long-standing debates concerning the origin and consequences of the severe and apparently global climate anomalies observed from c.536–550 CE, which began with recognition of the "mystery cloud" of 536 CE[40] observed in the Mediterranean basin. Under previous ice-core dating, it has been argued that this dust veil corresponded to an unknown tropical eruption dated 533–534 CE (±2)[41]. Using our revised timescales, we found at least two large volcanic eruptions around this period (Fig. 5). A first – apparently NH, eruptive episode in 535 or early 536 CE – injected large amounts of sulfate and ash into the atmosphere. Geochemistry of tephra filtered from the NEEM-2011-S1 ice core at a depth corresponding to 536 CE indicated multiple North American volcanoes as likely candidates for a combined volcanic signal (Extended Data Fig. 5, Methods, Supplementary Data). Historical observations (Extended Data Table 3) identified atmospheric dimming as early as March 24, 536, lasting up to 18 months. Summer 536 appeared exceptionally cold in almost all tree-ring reconstructions in the extra-tropical NH from N-America[34], over Europe[35,42,43] to Asia[44]. Depending upon reconstruction method, European summer temperatures in 536 CE dropped 1.6-2.5°C relative to the previous 30-year average[3]. A second eruptive episode in 539 or 540 CE, identified in both Greenland and Antarctica ice-core records and hence likely tropical in origin, resulted in up to 10% higher global aerosol loading than the Tambora 1815 eruption reconstructed from our bipolar sulfate records. Summer temperatures consequently dropped again, by 1.4-2.7°C in Europe in 541 CE[3], and cold temperatures persisted in the NH until almost 550 CE[3,33,34,42] (Figs. 2, 3, 5). This provides a notable environmental context to widespread famine and the great Justinian Plague 541-543 CE that was responsible for decimating populations in the Mediterranean and potentially China[45,46]. While certain climatic conditions (e.g., wet summers) have been linked to plague outbreaks in the past[47], a direct causal connection of these two large volcanic episodes and subsequent cooling to crop failures and outbreaks of famines and plagues is difficult to prove[33].

However, the exact delineation of two of the largest volcanic signals – with exceptionally strong and prolonged NH cooling; written evidence of famines and pandemics; as well as socio-economic decline observed in Mesoamerica ("Maya Hiatus"[48]), Europe, and Asia – supports the idea that the latter may be causally associated with volcanically-induced climatic extremes.

Detailed study of major volcanic events during the 6th century (Fig. 5) and an assessment of post-volcanic cooling throughout the past 2,500 years using stacked tree-ring records and regional temperature reconstructions (Fig. 4, Extended Data Fig. 4) demonstrated that large eruptions in the tropics and high latitudes were primary drivers of interannual-to-decadal NH temperature variability. The new ice-core chronologies imply that previous multi-proxy reconstructions of temperature that include ice-core records[2-4] have diminished high-to-mid-frequency amplitudes and must be updated to accurately capture the timing and full amplitude of paleoclimatic variability. By creating a volcanic forcing index independent of but consistent with NH tree-ring temperature anomalies, we provide an essential step to advance understanding of external forcing on natural climate variability during the past 2,500 years. With the expected detection of additional rapid $\Delta^{14}C$ enrichment events from ongoing efforts in annual resolution ^{14}C tree-ring analyses[49], there will be future opportunities to further constrain ice-core dating throughout the Holocene and develop a framework of precisely dated, globally synchronized proxies of past climate variability and external climate forcing.

1 Robock, A. Volcanic eruptions and climate. *Rev Geophys* **45**, doi: 1029/2007rg000232 (2007).

2 Hanhijarvi, S., Tingley, M. P. & Korhola, A. Pairwise comparisons to reconstruct mean temperature in the Arctic Atlantic Region over the last 2,000 years. *Clim Dynam* **41**, 2039-2060 (2013).

3 PAGES 2k Consortium Continental-scale temperature variability during the past two millennia. *Nature Geoscience* **6**, doi: 10.1038/Ngeo1834 (2013).

4 Mann, M. E. *et al.* Proxy-based reconstructions of hemispheric and global surface temperature variations over the past two millennia. *P Natl Acad Sci USA* **105**, 13252-13257, (2008).

5 Usoskin, I. G. A history of solar activity over millenia. *Living Rev Sol. Phys* **10,** doi:10.12942/lrsp-2013-1 (2013).

6 Gao, C. C., Robock, A. & Ammann, C. Volcanic forcing of climate over the past 1500 years: An improved ice core-based index for climate models. *J Geophys Res-Atmos* **113**, doi: D23111 10.1029/2008jd010239 (2008).

7 Crowley, T. J. & Unterman, M. B. Technical details concerning development of a 1200-yr proxy index of global volcanism. *Earth System Science Data* **5,** 187-197 (2013).

8 Mann, M. E., Fuentes, J. D. & Rutherford, S. Underestimation of volcanic cooling in tree-ring-based reconstructions of hemispheric temperatures. *Nat Geosci* **5**, 202-205 (2012).

9 Mann, M. E., Rutherford, S., Schurer, A., Tett, S. F. B. & Fuentes, J. D. Discrepancies between the modeled and proxy-reconstructed response to volcanic forcing over the past millennium: Implications and possible mechanisms. *J Geophys Res-Atmos* **118**, 7617-7627 (2013).

10 Schurer, A. P., Hegerl, G. C., Mann, M. E., Tett, S. F. B. & Phipps, S. J. Separating Forced from Chaotic Climate Variability over the Past Millennium. *J Climate* **26**, 6954-6973 (2013).

11 Anchukaitis, K. J. *et al.* Tree rings and volcanic cooling. *Nat Geosci* **5**, 836-837 (2012).

12 Büntgen, U. *et al.* Extraterrestrial confirmation of tree-ring dating. *Nat Clim Change* **4**, 404-405 (2014).

13 Esper, J., Büntgen, U., Luterbacher, J. & Krusic, P. J. Testing the hypothesis of post-volcanic missing rings in temperature sensitive dendrochronological data. *Dendrochronologia* **31**, 216-222 (2013).

14 D'Arrigo, R., Wilson, R. & Anchukaitis, K. J. Volcanic cooling signal in tree ring temperature records for the past millennium. *J Geophys Res-Atmos* **118**, 9000-9010 (2013).

15 Plummer, C. T. *et al.* An independently dated 2000-yr volcanic record from Law Dome, East Antarctica, including a new perspective on the dating of the 1450s CE eruption of Kuwae, Vanuatu. *Clim Past* **8**, 1929-1940 (2012).

16 Sigl, M. *et al.* A new bipolar ice core record of volcanism from WAIS Divide and NEEM and implications for climate forcing of the last 2000 years. *J Geophys Res-Atmos* **118**, 1151-1169 (2013).

17 Sigl, M. *et al.* Insights from Antarctica on volcanic forcing during the Common Era. *Nat Clim Change* **4**, 693-697 (2014).

18 Esper, J. *et al.* European summer temperature response to annually dated volcanic eruptions over the past nine centuries. *B Volcanol* **75**, doi: 10.1007/S00445-013-0736-Z (2013).

19 Douglass, D. H. & Knox, R. S. Climate forcing by the volcanic eruption of Mount Pinatubo. *Geophys Res Lett* **32**, L05710, doi: 10.1029/2004gl022119 (2005).

20 Baillie, M. G. L. Proposed re-dating of the European ice core chronology by seven years prior to the 7th century AD. *Geophys Res Lett* **35**, L15813, doi: 10.1029/2008gl034755 (2008).

21 Baillie, M. G. L. & McAneney, J. Tree ring effects and ice core acidities clarify the volcanic record of the 1st millennium. *Clim. Past* **11**, 105-114 (2015).

22 Miyake, F., Nagaya, K., Masuda, K. & Nakamura, T. A signature of cosmic-ray increase in AD 774-775 from tree rings in Japan. *Nature* **486**, 240-242 (2012).

23 Miyake, F., Masuda, K. & Nakamura, T. Another rapid event in the carbon-14 content of tree rings. *Nat Commun* **4**, doi: 10.1038/Ncomms2783 (2013).

24 Usoskin, I. G. *et al.* The AD775 cosmic event revisited: the Sun is to blame. *Astron Astrophys* **552**, doi: 10.1051/0004-6361/201321080 (2013).

25 Jull, A. J. T. *et al.* Excursions in the 14C record at A. D. 774-775 in tree rings from Russia and America. *Geophys Res Lett* **41**, 3004-3010 (2014).

26 Güttler, D. *et al.* Rapid increase in cosmogenic 14C in AD 775 measured in New Zealand kauri trees indicates short-lived increase in 14C production spanning both hemispheres. *Earth Planet. Sci. Lett.* **411**, 290-297 (2015).

27 Miyake, F. *et al.* Cosmic ray event of AD 774-775 shown in quasi-annual 10 Be data from the Antarctic Dome Fuji ice core. *Geophys. Res. Lett.* **42**, 84-89 (2015).

28 Webber, W. R., Higbie, P. R. & McCracken, K. G. Production of the cosmogenic isotopes H-3, Be-7, Be-10, and Cl-36 in the Earth's atmosphere by solar and galactic cosmic rays. *J Geophys Res-Space* **112**, A10106, doi: 10.1029/2007ja012499 (2007).

29 Masarik, J. & Beer, J. An updated simulation of particle fluxes and cosmogenic nuclide production in the Earth's atmosphere. *J Geophys Res-Atmos* **114**, D11103, doi: 10.1029/2008jd010557 (2009).

30 Vinther, B. M. *et al.* A synchronized dating of three Greenland ice cores throughout the Holocene. *J Geophys Res-Atmos* **111**, D13102, doi: 10.1029/2005jd006921 (2006).

31 Lavigne, F. *et al.* Source of the great A.D. 1257 mystery eruption unveiled, Samalas volcano, Rinjani Volcanic Complex, Indonesia. *P Natl Acad Sci USA* **110**, 16742-16747 (2013).

32 Winstrup, M. *et al.* An automated approach for annual layer counting in ice cores. *Clim Past* **8**, 1881-1895 (2012).

33 McCormick, M. *et al.* Climate Change during and after the Roman Empire: Reconstructing the Past from Scientific and Historical Evidence. *J Interdiscipl Hist* **43**, 169-220 (2012).

34 Salzer, M. W. & Hughes, M. K. Bristlecone pine tree rings and volcanic eruptions over the last 5000 yr. *Quaternary Res* **67**, 57-68 (2007).

35 Esper, J., Duthorn, E., Krusic, P. J., Timonen, M. & Buntgen, U. Northern European summer temperature variations over the Common Era from integrated tree-ring density records. *J Quaternary Sci* **29**, 487-494 (2014).

36 Crowley, T. J. Causes of climate change over the past 1000 years. *Science* **289**, 270-277 (2000).

37 Driscoll, S., Bozzo, A., Gray, L. J., Robock, A. & Stenchikov, G. Coupled Model Intercomparison Project 5 (CMIP5) simulations of climate following volcanic eruptions. *J Geophys Res-Atmos* **117**, D17105, doi: 10.1029/2012jd017607 (2012).

38 Schneider, D. P., Ammann, C. M., Otto-Bliesner, B. L. & Kaufman, D. S. Climate response to large, high-latitude and low-latitude volcanic eruptions in the Community Climate System Model. *J Geophys Res-Atmos* **114**, D15101, doi: 10.1029/2008jd011222 (2009).

39 Zanchettin, D. *et al.* Inter-hemispheric asymmetry in the sea-ice response to volcanic forcing simulated by MPI-ESM (COSMOS-Mill). *Earth Syst Dynam* **5**, 223-242 (2014).

40 Stothers, R. B. Mystery Cloud of Ad-536. *Nature* **307**, 344-345 (1984).

41 Larsen, L. B. *et al.* New ice core evidence for a volcanic cause of the AD 536 dust veil. *Geophys Res Lett* **35**, L04708, doi: 10.1029/2007gl032450 (2008).

42 Büntgen, U. *et al.* 2500 Years of European Climate Variability and Human Susceptibility. *Science* **331**, 578-582 (2011).

43 Esper, J. *et al.* Orbital forcing of tree-ring data. *Nat Clim Change* **2**, 862-866 (2012).

44 D'Arrigo, R. *et al.* 1738 years of Mongolian temperature variability inferred from a tree-ring width chronology of Siberian pine. *Geophys Res Lett* **28**, 543-546 (2001).

45 Zhang, Z. B. *et al.* Periodic climate cooling enhanced natural disasters and wars in China during AD 10-1900. *P Roy Soc B-Biol Sci* **277**, 3745-3753 (2010).

46 Stothers, R. B. Volcanic dry fogs, climate cooling, and plague pandemics in Europe and the Middle East. *Climatic Change* **42**, 713-723 (1999).

47 Stenseth, N. C. *et al.* Plague dynamics are driven by climate variation. *P Natl Acad Sci USA* **103**, 13110-13115 (2006).

48 Dull, R. A. Evidence for forest clearance, agriculture, and human-induced erosion in Precolumbian El Salvador. *Ann Assoc Am Geogr* **97**, 127-141 (2007).

49 Taylor, R. E. & Southon, J. Reviewing the Mid-First Millennium BC C-14 "warp" using C-14/bristlecone pine data. *Nucl Instrum Meth B* **294**, 440-443 (2013).

Supplementary Information is available in the online version of the paper.

Acknowledgements. We thank the many persons involved in logistics, drill development and drilling, and ice-core processing and analysis in the field and our laboratories. This work was supported by the U.S. National Science Foundation (NSF). The authors appreciate support of the WAIS Divide Science Coordination Office (M. Twickler and J. Souney) for collection and distribution of the WAIS Divide ice core; Ice Drilling and Design and Operations (K. Dahnert) for drilling; the National Ice Core Laboratory (B. Bencivengo) for curating the core; Raytheon Polar Services (M. Kippenhan) for logistics support in Antarctica; and the 109th New York Air National Guard for airlift in Antarctica. NEEM is directed and organized by the Center of Ice and Climate at the Niels Bohr Institute and U.S. NSF, Office of Polar Programs. It is supported by funding agencies and institutions in Belgium (FNRS-CFB and FWO), Canada (NRCan/GSC), China (CAS), Denmark (FIST), France (IPEV, CNRS/INSU, CEA and ANR), Germany (AWI), Iceland (RannIs), Japan (NIPR), Korea (KOPRI), The Netherlands (NWO/ALW), Sweden (VR), Switzerland (SNF), United Kingdom (NERC), and the USA (U.S. NSF, Office of Polar Programs). We thank B. Nolan, O. Amir, K. D. Pang, M. McCormick, and B. Rossignol for assistance in surveying and/or interpreting the historical evidence. We thank S. Kuehn for commenting on possible correlations for the tephra. A. Aldahan and G. Possnert are thanked for their support in the NGRIP ^{10}Be preparations and measurements at the Department of Earth Sciences and the Tandem laboratory at Uppsala University. We gratefully acknowledge R.r Kreidberg for his editorial advice.

The following individual grants supported this work: NSF/OPP grants 0839093, 0968391, and 1142166 to J.R.M. for development of the Antarctic ice core records and NSF/OPP grants 0909541, 1023672, and 1204176 to J.R.M. for development of the Arctic ice core records. M.W. was funded by the Villum Foundation. K.C.W. was funded by NSF/OPP grants 0636964 and 0839137. M.W.C. and T.W. were funded by NSF/OPP grants 0839042 and 0636815. F.L. was funded by the Yale Climate &

Energy Institute, Initiative for the Science of the Human Past at Harvard, and Rachel Carson Center for Environment and Society of the Ludwig-Maximilians-Universität (LMU Munich). C.K. was funded by a Marie Curie CIG. M. Sa. was funded by NSF grant ATM 1203749. R.M. was funded by the Swedish Research Council (DNR2013-8421). The division of Climate and Environmental Physics, Physics Institute, University of Bern, acknowledges financial support by the SNF and the Oeschger Centre.

Author Contributions. M.Si. designed the study with input from J.R.M., M.W., G.P., and F.L. The manuscript was written by M.Si., M.W., F.L., and J.R.M., with contributions from K.C.W., G.P., U.B., B.V. in interpretation of the measurements. Ice-core chemistry measurements were performed by J.R.M., M.Si., O.J.M., N.C., D.R.P. (NEEM, B40, TUNU2013), and by S.S., H.F., R.Mul. (NEEM). K.C.W., T.E.W., and M.C. completed ice core ^{10}Be measurements. F.M. and R.Mus. were responsible for the NGRIP ice core ^{10}Be measurements. M.Si., M.W., B.V., and J.R.M. analyzed ice-core data and developed age models. F.L. and C.K. analyzed historical documentary data. G.P and J.R.P. performed ice-core tephra analysis and data interpretation. U.B. and M.Sa. contributed tree-ring data. D.D.-J., B.V., J.P.S., S.K., and O.J.M. were involved in drilling of the NEEM ice core. TUNU2013 was drilled by M.Si., N.C. and O.J.M., and the B40 ice core was drilled by S.K. and made available for chemistry measurements. D.D.-J. and J.P.S. were responsible for NEEM project management, sample distribution, logistics support, and management. All authors contributed toward improving the final manuscript.

Author Information. The authors declare no competing financial interests. Correspondence and requests for materials should be addressed to M.Si. (msigl@dri.edu).

Figure 1 | Annual ^{10}Be ice-core records and post-volcanic cooling from tree rings for selected time periods using existing ice-core chronologies. a) Superposed epoch analysis for the seven largest volcanic signals in NEEM-2011-S1 between 78 and 1000 CE and for the 10 largest eruptions between 1250 and 2000 CE, respectively[16]. Shown are growth anomalies from a multi-centennial,

temperature-sensitive tree-ring composite (N-Tree[42,43,76-78], Methods) 10 years after the year of volcanic sulfate deposition at NEEM ice core site in Greenland (GICC05 timescale), relative to the level five years prior to sulfate deposition; **b)** annually resolved ^{10}Be concentration records (1σ measurement uncertainty) from WDC, TUNU2013, NGRIP, and NEEM-2011-S1 ice cores on their original timescales and annually resolved Δ^{14}C series from tree-ring records between 755-795 CE[22,24], with arrows representing the suggested time shifts for synchronization; estimated relative age uncertainty for TUNU2013 at this depth interval from volcanic synchronization with NEEM-2011-S1 is ±1 year; **c)** annually resolved ^{10}Be concentration record from NEEM-2011-S1 ice core on its original timescale and annually resolved Δ^{14}C series from tree rings between 980-1010 CE[23].

Figure 2 | Re-dated ice-core, non-sea-salt sulfur records from Greenland and Antarctica in relation to growth anomalies in the N-Tree composite. a) Upper panel: Ice-core, non-sea-salt sulfur (nssS) records from Greenland (NEEM, NEEM-2011-S1) on the NS1-2011 timescale between 500 BCE and 1300 CE, with identified layer of Tianchi tephra[67] highlighted (orange star). Calendar years are given for the start of volcanic sulfate deposition. Events used as fixed age markers to constrain the dating (i.e., 536, 626, 775, 939, and 1258) are indicated (purple stars). Annually resolved ^{10}Be concentration record (green) from NEEM-2011-S1 encompassing the two Δ^{14}C excursion events in trees from 775 and 994; middle panel: tree-ring growth anomalies (relative to 1000-1099 CE) for the N-Tree composite[42,43,76-78]; lower panel: nssS records from Antarctica (WDC, B40) on the WD2014 timescale and annually resolved ^{10}Be concentrations from WDC; **b**) superposed epoch analysis for the 28 largest volcanic signals during the past 2,500 years. Tree-ring growth anomalies relative to the timing of reconstructed sulfate deposition in Greenland (NS1-2011) are shown for 1250 to 2000 CE and 500 BCE to 1250 CE.

Figure 3 | Global volcanic aerosol forcing and NH temperature variations for the past 2,500 years. **a)** 2,500 year record of tree-growth anomalies (N-Tree[42,43,76-78]; relative to 1000-1099 CE) and reconstructed summer temperature anomalies for Europe and Arctic[3] ; 40 coldest single years and

12 coldest decades based on N-Tree are indicated; **b**) reconstructed global volcanic aerosol forcing from bipolar sulfate composite records from tropical (bipolar), NH, and SH eruptions. Total (i.e., time integrated) forcing values are calculated by summing the annual values for the duration of volcanic sulfur deposition. 40 largest volcanic signals are indicated, and ages are given for events representing atmospheric sulfate loading exceeding Tambora 1815.

Figure 4 | Post-volcanic cooling. Superposed composites (time segments from selected periods in the Common Era positioned so that the years with peak negative forcing are aligned) of the JJA temperature response to: **a)-c)** 24 largest eruptions (>Pinatubo 1991) for three regional reconstructions in Europe[3,35,42]; **d)-f)** 19 largest tropical eruptions; **g)** five largest NH eruptions; **h)** eruptions with negative forcing larger than Tambora 1815 for Central Europe and **i)** for Northern Europe (note the different scale for g-i); shown are JJA temperature anomalies (°C) for 15 years after reconstructed volcanic peak forcing, relative to the five years before the volcanic eruption. Dashed lines present two times the standard error of the mean (2 SEM) of the temperature anomalies associated with the multiple eruptions. 5-year average post-volcanic temperatures are shown for each reconstruction (lag 0 to lag +4 yrs, gray shading).

Figure 5 | Volcanism and temperature variability during the Migration Period (500-705 CE). Upper panel: Ice-core non-sea-salt sulfur (nssS) records from Greenland (NEEM-2011-S1, TUNU2013). Insets give translations of historical documents describing observation of post-volcanic atmospheric effects in 536-537 and 626-627 CE. Calendar years for five large eruptions are given for the start of volcanic sulfate deposition; middle panel: reconstructed N-Tree growth anomalies (relative to 1000-1099 CE) and occurrence of frost rings in North American bristlecone pine tree-ring records; lower panel: nssS records from Antarctica (WDC, B40) on the WD2014 timescale; attribution of the sulfur signals to bipolar, NH, and SH events based on the timing of deposition on the two independent timescales is indicated by shading.

Methods

Ice cores. This study included new and previously described ice-core records from five drilling sites (Extended Data Fig. 1, Supplementary Data). The upper 577 m of the 3,405 m WAIS Divide (WDC) core from central West Antarctica and a 410 m intermediate-length core (NEEM-2011-S1) drilled in 2011 close to the 2,540 m North Greenland Eemian Ice Drilling (NEEM)[50] ice core previously have been used to reconstruct sulfate deposition in both polar ice sheets[16]. These coring sites are characterized by relatively high snowfall (~200 kg m^{-2} yr^{-1}) and have comparable elevation, latitude, and deposition regimes. WDC and NEEM-2011-S1 provided high-resolution records that allowed annual-layer dating based on seasonally varying impurity content[16]. New ice-core analyses included the upper 514 m of the main NEEM core used to extend the record of NEEM-2011-S1 to cover the past 2,500 years, as well as B40 drilled in 2012 in Dronning Maud Land in East Antarctica and TUNU2013 drilled in 2013 in Northeast Greenland – both characterized by lower snowfall rates (~70-100 kg m^{-2} yr^{-1}). Volcanic sulfate concentration from B40 had been reported previously for the past 2,000 years[17], but we extended measurements to 200 m depth to cover the past 2,500 years.

High-resolution, ice-core aerosol analyses. Ice-core analyses were performed at the Desert Research Institute (DRI) using 55 to 100 cm long, longitudinal ice core sections (33 x 33 mm wide). The analytical system for continuous analysis included two Element2 (Thermo Scientific) high-resolution inductively coupled plasma mass spectrometers (HR-ICP-MS) operating in parallel for measurement of a broad range of ~35 elements; an SP2 (Droplet Measurement Technologies) instrument for black carbon (BC) measurements; and a host of fluorimeters and spectrophotometers for ammonium (NH_4^+), nitrate (NO_3^-), hydrogen peroxide (H_2O_2), and other chemical species. All measurements were exactly co-registered in depth, with depth resolution typically less than 10-15 mm[51-53]. We corrected total sulfur (S) concentrations for the sea-salt-sulfur contribution using sea-salt-Na concentrations[16]. Measurements included TUNU2013 and NEEM (400-515 m) in Greenland, and B40 in Antarctica (Extended Data Fig. 1). Gaps (i.e., ice not allocated to DRI) in the high-resolution sulfur data of the NEEM core were filled with ~4 cm resolution discrete sulfate

454 measurements using fast ion-chromatography techniques[54] performed in the field between 428 and
455 506 m depth.

456 Independent analyses of the upper part of the NEEM main core were performed in the field
457 using a continuous flow analysis (CFA) system[55] recently modified to include a new melter head
458 design[56]. Ca^{2+}, NH_4^+, and H_2O_2 were analyzed by fluorescence spectroscopy; Na^+ and NO_3^- by
459 absorption spectroscopy; conductivity of the meltwater by a micro flow cell (Amber Science Inc.);
460 and a particle detector (Abakus, Klotz) was used for measuring insoluble dust particle concentrations
461 and size distribution[57]. Effective depth resolution typically was better than 20 mm. Measurements
462 were exactly synchronized in depth using a multicomponent standard solution; the accuracy of the
463 depth assignment for all measurements typically was better than 5 mm.

464 **High-resolution measurements of ^{10}Be in ice cores using accelerator mass spectrometry (AMS).**
465 Samples from the NEEM-2011-S1, WDC, NGRIP, and TUNU2013 ice cores encompassing the time
466 period of the Δ^{14}C anomalies from tree-ring records[12,22-25] were used for ^{10}Be analysis
467 (Supplementary Data). NEEM-2011-S1 and WDC were sampled in exact annual resolution, using the
468 maxima (minima in WDC) of the annual cycles of Na concentrations to define the beginning of the
469 calendar year[16]. NGRIP was sampled at a constant resolution of 18.3 cm providing an age resolution
470 of about one year. Similarly, TUNU2013 was sampled in quasi-annual resolution according to the
471 average annual-layer thickness expected at this depth based on prior volcanic synchronization to
472 NEEM-2011-S1. The relative age uncertainty for TUNU2013 with respect to the dependent NEEM-
473 2011-S1 chronology at this depth is assumed to be ±1 year at most given a distinctive match for
474 selected volcanic trace elements in both ice core records (752-764 C.E., NS1-2011 timescale). Sample
475 masses ranged between 100 and 450 g, resulting in median overall quantification uncertainties of
476 less than 4–7%. The ^{10}Be/^{9}Be ratios of samples and blanks were measured relative to well-
477 documented ^{10}Be standards[13] by AMS at Purdue's PRIME laboratory (WDC, NEEM-2011-S1,
478 Tunu2013) and Uppsala University (NGRIP)[58,59]. Results were corrected for an average blank ^{10}Be/^{9}Be
479 ratio, corresponding to corrections of 2–10% of the measured ^{10}Be/^{9}Be ratios.

Annual-layer dating using the StratiCounter algorithm. For annual-layer interpretation, we used DRI's broad-spectrum aerosol concentration data from WDC (188–577 m), NEEM-2011-S1 (183–411 m), and NEEM (410–515 m), as well as NEEM aerosol concentration data (183–514 m) from the field-based CFA system. The original timescale for NEEM-2011-S1 was based on volcanic synchronization to the NGRIP sulfate record on the GICC05 timescale and annual-layer interpretation between the volcanic age markers, while WDC previously was dated by annual-layer counting[16].

Parameters with strong intra-annual variability included tracers of sea salt (e.g., Na, Cl, Sr), dust (e.g., Ce, Mg, insoluble particle concentration), and marine biogenic emissions such as non-sea-salt sulfur (nssS). Tracers of biomass-burning emissions, such as BC, NH_4^+, and NO_3^-, also showed strong seasonal variations in deposition during pre-industrial times[16,60,61]. Datasets used for annual layer interpretation are provided in Extended Data Table 1. For NEEM-2011-S1, the final database used for annual-layer dating included 13 parameters and the ratio of nssS/Na. For WDC, the final database included five parameters and the ratio of nssS/Na. For NEEM (410-515 m depth), the final database included eight parameters (Na^+, Ca^{2+}, NH_4^+, H_2O_2, NO_3^-, conductivity, insoluble particle concentrations, and ECM[62]) from the field-based measurements and eleven parameters (Na, Cl, Mg, Mn, Sr, nssS, nssS/Na, nssCa, BC, NO_3^-, NH_4^+) from the DRI system.

We focused here on the time period prior to the large volcanic eruption of Samalas in 1257 CE[31], clearly detectable as an acidic peak in both ice-core records, and consequently started annual-layer counting of NEEM-2011-S1, NEEM, and WDC at the depth of the corresponding sulfur signal. For the time period 1257 CE to present, ice-core chronologies were constrained by numerous historic eruptions and large sulfate peaks showing a strong association to Northern Hemisphere (NH) cooling events as indicated by tree-ring records[16].

We applied the StratiCounter layer-detection algorithm[32] to the multi-parameter aerosol concentration records (n=14 for NEEM-2011-S1; n=6 for WDC; n=8 for NEEM <410 m; n=19 for NEEM >410 m) to objectively determine the most likely number of annual layers in the ice cores along with

505 corresponding uncertainties. The StratiCounter algorithm is based on statistical inference in Hidden
506 Markov Models (HMMs), and it determines the maximum likelihood solution based on the annual
507 signal in all aerosol records in parallel. Some of these displayed a high degree of similarity, so we
508 weighted these records correspondingly lower. The algorithm was run step-wise down the core,
509 each batch covering approximately 50 years, with a slight overlap. All parameters for the statistical
510 description of a mean layer and its inter-annual variability in the various aerosol records were
511 determined independently for each batch as the maximum likelihood solution. The algorithm
512 simultaneously computes confidence intervals for the number of layers within given sections,
513 allowing us to provide uncertainty bounds on the number of layers between selected age-marker
514 horizons (Extended Data Table 2).

515 Annual-layer detection in the NEEM main core below 410 m was made more difficult by
516 frequent occurrence of small gaps in the two independent high-resolution aerosol data sets.
517 Depending on the parameter, data gaps from the CFA field measurements accounted for up to 20%
518 of the depth range between 410 and 515 m, but the combined aerosol records from both analyses
519 provided an almost complete aerosol record with 96% data coverage. As this was the first time that
520 the StratiCounter algorithm was used simultaneously on data records from two different melt
521 systems, with different characteristics and lack of exact co-registration, we also manually
522 determined annual layers below 410 m using the following approaches: one investigator used Na
523 and nssCa concentrations and the ratio of nssS/Na (from DRI analysis) as well as Na^+ and insoluble
524 particle concentrations (from CFA analysis) as primary dating parameters. BC, NH_4^+, nssS, and
525 conductivity were used as secondary dating parameters where annual-layer interpretation was
526 ambiguous. A second investigator used DRI's Na, Ca, BC, NH_4^+ and CFA Na^+, Ca^{2+}, NH_4^+. The annual-
527 layer interpretation of the NEEM core between 410 and 514 m from investigator 1 was within the
528 interpretation uncertainties of the StratiCounter output, from which it differed less than a single
529 year over the majority of this section, and it differed from independently counted timescales (e.g.,

GICC05)[62] by on average less than three years (Extended Data Fig. 2). We decided to use this set of layer counts for the resulting timescale.

New ice-core chronologies (NS1-2011, WD2014). We defined the depth of NEEM-2011-S1 containing the maximum ^{10}Be concentration as the year 775 CE. Relative to this constraint, the maximum likelihood ages for three large volcanic sulfate peaks were within ±1 year of documented historical reports from early written sources of prominent and sustained atmospheric dimming observed in Europe and/or Asia (Extended Data Table 3, Supplementary Data). Automated-layer identification for NEEM-2011-S1 was therefore constrained by tying the respective ice-core volcanic signals to the corresponding absolute historically-dated ages of 536, 626, and 939 CE (Extended Data Table 2) – thereby creating a new ice-core timescale (NS1-2011). The volcanic sulfur signal corresponding to the eruption of Samalas believed to have occurred in late 1257[31] was constrained to 1258 CE to account for several months' delay in sulfate deposition in the high latitudes. Before 86 CE (the bottom depth of NEEM-2011-S1), the NS1-2011 timescale was extended using the manually-derived annual-layer interpretation of the combined NEEM aerosol data sets back until 500 BCE (Fig. 2).

In NS1-2011 we did not attribute acid layers to the historical eruptions Vesuvius 79 and Hekla 1104, due to a lack of corroborative tephra at these depths in this and a previous study[63]. Possible Vesuvius tephra was reported from the Greenland Ice Sheet Project (GRIP) ice core at 429.3 m depth[64], but in view of the new annual-layer dating results (Extended Data Fig. 3), we concluded that this layer dates to 87/88 CE. Furthermore, volcanic sulfate deposition values for the corresponding event show a strong spatial gradient over Greenland with highest values in NW Greenland[16] and lowest in Central and South Greenland[65], favoring the attribution of a volcanic source from the high latitudes. Documentary sources (Supplementary Data) also suggest that the main vector of ash transport following the Vesuvius 79 CE eruption was toward the eastern Mediterranean[66].

For WDC, we do not have other sufficiently well-determined age constraints besides the rapid ^{10}Be increase in 775 CE and the sulfur signal of the Samalas 1257 eruption. Therefore, no additional constraints were used when creating the new ice-core timescale ("WD2014") from the StratiCounter annual-layer interpretation back to 396 BCE.

Depth-age information for six distinctive marker horizons in Greenland is given, and five of these horizons were used to constrain NS1-2011 (Extended Data Table 3). Similarly, depth information, the number of annual layers, and 95% confidence intervals between distinctive volcanic marker horizons are given for NEEM, NEEM-2011-S1, and WDC, supporting attribution of these ice-core signals to eruptions in the low latitudes with bipolar sulfate deposition.

Evaluation of NS1-2011 using independent age information. We evaluated timescale accuracy using additional distinctive age markers not used during chronology development:

1) Tephra from the eruption of Changbaishan/Tianchi (China)[67] was detected in NEEM-2011-S1 in 946–947 CE, in agreement with widespread documentary evidence of an eruption in that region in winter 946/47 CE[68]also supported by a high-precision ^{14}C wiggle-match age of 946 ± 3 CE obtained from a tree killed during this eruption[68].
2) The rapid increase of ^{10}Be of the 994 event occurred in NEEM-2011-S1 in 993 CE, consistent with Δ^{14}C from Japanese tree rings showing that the rapid increase in radionuclide production took place between the NH growing seasons of 993 and 994 CE[23].
3) To assess the accuracy of the NS1-2011 timescale prior to the earliest age marker at 536 CE, we compiled an independent time series of validation points, featuring years with well dated historical reports of atmospheric phenomena associated with high-altitude volcanic dust and/or aerosols (Supplementary Data) as known from modern observations to occur after major eruptions (e.g., Krakatau, 1883). These phenomena include diminished sunlight, discoloration of the solar disk, solar coronae (i.e., Bishop's Rings), and deeply red twilights (i.e., volcanic sunsets)[69,70]. Thirty-two events met our criteria as validation points for the pre-

536 CE NS1-2011 timescale. For the earliest in 255 BCE, it was reported in Babylonia that "the disk of the sun looked like that of the moon"[73]. For the latest in 501 CE, it was reported in North China that "the Sun was red and without brilliance"[74]. We found that NEEM volcanic event years (including both NEEM and NEEM-2011-S1 data) occurred closely in time (i.e., within a conservative ±3 year margin) to 24 (75.0%) of our validation points (Extended Data Figure 2). To assess whether this association arose solely by chance, we conducted a Monte Carlo equal means test with 1,000,000 iterations (Supplementary Data) and found that the number of volcanic event years within ±3 years of our validation points was significantly greater than expected randomly ($p<0.001$). A significant association was also observed ($p<0.001$) when using less conservative error margins (±1/±2 years) and when excluding any historical observations with less certainty of a volcanic origin (Supplementary Data). When placing volcanic event years on the original GICC05 timescale, we did not observe any statistically significant association with our independent validation points

Potential causes of a previous ice-core dating bias. Interpretation of annual layers in ice cores is subject to accumulating age uncertainty due to ambiguities in the underlying ice-core profiles[30,73]. Bias in existing chronologies may arise from several factors, including: 1) low effective resolution of some ice core measurements (NGRIP, GRIP); 2) use of only single (or few) parameters for annual-layer interpretation (GRIP, Dye-3); 3) intra-annual variations in various ice-core parameters falsely interpreted as layer boundaries (e.g., caused by summer melt in Dye-3)[74]; 4) use of tephra believed to originate from the 79 CE Vesuvian eruption[64] as a fixed reference horizon to constrain the Greenland ice-core dating[30]; 5) use of manual-layer interpretation techniques that may favor interpretations consistent with *a priori* knowledge or existing chronologies (WDC)[16,21].

Volcanic synchronization of B40, TUNU2013, and NGRIP to WDC and NEEM. Two high-resolution sulfur ice-core records (TUNU2013, Greenland and B40, Antarctica) were synchronized to NEEM-2011-S1 and WDC, respectively, using volcanic stratigraphic age markers[17] with relative age uncertainty between the tie-points estimated to not exceed ±2 years. The NGRIP sulfate record

606 measured at 4 cm depth resolution[15] similarly was synchronized to NS1-2011 using 124 volcanic tie-
607 points between 226 and 1999 CE. During the time period with no sulfur record yet available for WDC
608 (before 396 BCE), a tentative chronology for B40 was derived by linearly extrapolating mean annual-
609 layer thickness for B40 as derived from the synchronization to WDC between the earliest volcanic
610 match points.

611 **2,500 year global volcanic forcing ice-core index.** We constructed an index of global volcanic aerosol
612 forcing by (1) re-dating and extending to 500 BCE an existing reconstruction of sulfate flux from an
613 Antarctic ice-core array[17] by applying an area weighting of 80/20 between East Antarctica and West
614 Antarctica to B40 and WDC volcanic sulfate flux values, respectively; (2) compositing NGRIP and the
615 NEEM-2011-S1/NEEM sulfate flux records to a similar Greenland sulfate deposition composite back
616 to 500 BCE; (3) using established scaling functions[6,75] to estimate hemispheric sulfate aerosol loading
617 from both polar ice-core composites; and (4) scaling global aerosol loading to the total (i.e., time
618 integrated) radiative volcanic aerosol forcing following the Tambora 1815 eruption[7]. Since the NS1-
619 2011 and WD2014 timescales are independent of each other, the timing of bipolar events had to be
620 adjusted to follow a single timescale to derive a unified global volcanic forcing series. We chose NS1-
621 2011 as the reference chronology for most of the volcanic time series because this age model was
622 constrained and validated by more stratigraphic age markers than WD2014. WD2014 was used as
623 the reference chronology only between 150 and 450 CE, because of better data quality during that
624 time period. TUNU2013 was not included in the Greenland ice-core composite because annual-layer
625 thickness variability at this site is influenced strongly by glaciological processes, leading to relatively
626 large uncertainties in atmospheric sulfur-deposition determinations.

627 **NH tree-ring proxy records and temperature reconstructions.** To analyze the temporal coherence of
628 our new ice-core dates of volcanic peak forcing relative to the implied cooling response, we
629 compiled a composite record of multi-centennial records of tree growth at locations where
630 temperature is the main limiting factor. We selected all available NH tree-ring proxy records meeting

631 the following criteria: (1) covering >1,500 years; (2) no assumed chronological uncertainty; and (3)
632 strong relationship to local temperature and/or already demonstrated sensitivity to volcanic forcing.
633 In total, six records from three continents met the criteria[42,43,76-78], though we excluded the Avam-
634 Taymir record in N-Siberia[76] in order to give stronger weight to the two maximum latewood density
635 records[43,77], in many circumstances the preferred parameter to reconstruct annually resolved
636 temperature variations[35]. As various climatic and non-climatic parameters may influence sensitivity
637 of tree-growth to temperatures during the 20th century[79-81] we used the time period 1000-1099 CE as
638 a common baseline for standardizing tree growth anomalies among the five remaining records and
639 built a tree growth composite record "N-Tree" (z-scores) by averaging the individual records.
640 Correlations between "N-Tree" (N=5) and the average of three regional reconstructions for the
641 Arctic, Europe, and Asia (N>275)[3] between 1800 and 2000 are very high (R^2 = 0.78, N=201,
642 p<0.0001), suggesting that much of the large-scale variation in temperature is explained by these
643 few selected tree-ring records (Fig. 3). Three records in "N-Tree" cover the period from 138 BCE to
644 the present, thus allowing at least a qualitative assessment of the coherence of growth reduction
645 following large volcanic eruptions prior to the Common Era (Fig. 2, Extended Data Fig. 4).

646 To quantify the CE climate impact and investigate regional differences, we used tree-ring-based JJA
647 temperature reconstructions covering the past 2,000 years with demonstrated strong relationship (R
648 ≥ 0.5) to instrumental JJA temperature data[82] between 1901 and 2000. For regions where these
649 criteria were met by several reconstructions (e.g., Scandinavia), we limited the analysis to the most
650 recently updated reconstruction[35]. Three regional reconstructions from Central Europe [42], Northern
651 Europe[35], and Northern Siberia (Jamal, not shown)[83] as well as a continental-scale reconstruction for
652 Europe[3] met the criteria and were used to quantify the average response of summer temperature to
653 volcanic forcing during the Common Era (Figs. 3, 4).

654 **Superposed epoch analyses.** To assess tree-ring growth reduction and summer cooling following
655 large eruptions, we used superposed epoch analyses[84]. We selected all volcanic eruptions (28 events
656 in total, 24 CE events) with time-integrated volcanic forcing greater than -7.5 W m^{-2} (i.e., eruptions

larger than Pinatubo 1991) and aligned the individual segments of "N-Tree" and regional JJA temperature reconstructions relative to ice-core indicated peak forcing. Composite response was calculated for the average of the individual series (lag 0 to lag 10 or 15 years) relative to the average values five years prior to individual volcanic events (lag -5 to lag -1 year). 95% confidence intervals represent 2 SEM of the tree-growth (Extended Data Figure 4) and temperature anomalies (Figure 4) associated with the multiple eruptions.

Cryptotephra analyses of the 536 CE sample from NEEM-2011-S1. We analyzed samples from NEEM-2011-S1 for tephra between 326.73 and 328.06 m depth, corresponding to 531–539 CE (NS1-2011 timescale). Samples (200 to 500 g) were filtered, and elemental composition of recovered volcanic glass shards determined by electron microprobe analysis (EPMA) at Queen's University Belfast using established protocols[63,67,85] and secondary glass standards[86,87]. Between 326.73 and 327.25 m, large volume samples were cut at 8 cm depth resolution (≤0.5 yr) and with an average cross section of 26 cm^2. Between 327.25 and 328.06 m, the average cross section was 7 cm^2 and depth resolution 20 cm (~1 yr resolution). Tephra particles (n ≥17) were isolated from a sample of ice (327.17–327.25 m depth, 251 g) corresponding to the sulfate spike at 536 CE. The glass shards were heterogeneous in size (20–80 µm), morphology (platey, blocky, vesicular, microlitic), and geochemistry (andesitic, trachytic, rhyolitic). Individual shards had geochemical compositions that share affinities with volcanic systems in the Aleutian arc (Alaska)[88], Northern Cordilleran volcanic province (British Columbia)[89], and Mono-Inyo Craters area (California)[90,91] – indicating at least three synchronous eruptive events, all situated in western North America between 38 and 58°N (Extended Data Fig. 5; Supplementary Data).

Data: The code for the StratiCounter program is accessible at the github repository (http://www.github.com/maiwinstrup/StratiCounter); ice-core data (chemistry, including sulfur; ^{10}Be) and resulting timescales for the NEEM, NEEM-2011-S1, WDC, B40 and TUNU2013 are accessible at repository (to be determined); volcanic forcing reconstruction and sulfate records are

accessible at repository (to be determined); tree-ring records and temperature reconstructions are from Pages-2k Consortium (Database S1, S2) (http://www.nature.com/ngeo/journal/v6/n5/full/ngeo1797.html#supplementary-information).

Extended Data Figure 1 | Location of study sites. Map showing locations of the five ice-core (WDC, B40, NEEM, NGRIP and TUNU) used in this study and sites of temperature limited tree-ring chronologies (green) [42,43,76-78] and sites with annual $\Delta^{14}C$ measurements from tree-rings in the 8th century CE (red outline) are marked.

Extended Data Figure 2 | Volcanic dust veils from historical documentary sources in relation to NEEM. Time series of 32 independently-selected chronological validation points from well-dated historical observations of atmospheric phenomena with known association to explosive volcanism (e.g., diminished sunlight, discolored solar disk, solar corona or Bishop's Ring, red volcanic sunset) as reported in the Middle East, Mediterranean region, and China, prior to our earliest chronological age marker at 536 CE. Black lines represent the magnitude (scale on vertical y-axes) of annual sulfate deposition measured in NEEM (NEEM and NEEM-2011-S1 ice cores) from explosive volcanic events on the new NS1-2011 timescale. Red crosses depict the 24 (75%) historical validation points for which NEEM volcanic events occur within a conservative ±3 year uncertainty margin. Blue crosses represent the eight points for which volcanic events are not observed. The association between validation points and volcanic events is statistically significantly non-random at >99.9% confidence.

Extended Data Figure 3 | Timescale comparison. Age differences of the timescales **a)** NS1-2011 and GICC05 for the NEEM-2011-S1/NEEM ice cores and **b)** WD2014 and WDC06A-7 for WDC. Differences before 86 CE (the bottom age of NEEM-2011-S1) deriving from the annual-layer counting of the NEEM core are shown for major volcanic eruptions relative to the respective signals in NGRIP on the annual-layer counted GICC05 timescale. Marker events used for constraining the annual-layer dating (solid line) and for chronology evaluation (dashed lines) are indicated. Triangles mark volcanic

signals. Also indicated is the difference between WD2014 and the Antarctic ice-core chronology (AICC2012)[92], based on volcanic synchronization between the WDC and EDC96 ice cores.

Extended Data Figure 4 | Post-volcanic suppression of tree growth. Superposed epoch analysis for large volcanic eruptions using the **a)** 28 largest volcanic eruptions; **b)** 23 largest tropical eruptions; **c)** five largest NH eruptions; and **d)** eruptions larger than Tambora 1815 with respect to sulfate aerosol loading. Shown are growth anomalies of a multi-centennial tree-ring composite record (N-Tree) 10 years after the year of volcanic sulfate deposition, relative to the average of five years before the events. Shading indicates 95% confidence intervals (2 SEM) of the tree-ring growth anomalies associated with the multiple eruptions.

Extended Data Figure 5 | Major element composition for ice core tephra QUB-1859 and reference material. Shown are selected geochemistry data: (**a)** SiO_2 vs. total alkali (K_2O + Na_2O); **b)** FeO (total iron oxides) vs. TiO_2; **c)** SiO_2 vs. Al_2O_3; and **d)** CaO vs. MgO) from 11 shards extracted from the NEEM-2011-S1 ice core between 327.17 and 327.25 m depth, representing the age range 536.0–536.4 CE on the new, NS1-2011 timescale. Data for Late Holocene tephra from Mono Craters (California) are from the compilation by ref. 90 (all references in Methods); data for Aniakchak (Alaska) are from reference material published by ref. 88; and data for the early Holocene upper Finlay tephra , believed to be from the Edziza complex in the Upper Cordilleran Volcanic province (British Columbia), are from ref. 89.

Extended Data Table 1 | Ice-core dating. Parameters used for annual-layer interpretation. Parameters measured by the CFA system in the field are underlined. Stratigraphic age marker used to constrain annual-layer counting (*) and horizons used to evaluate the timescale (†).

Extended Data Table 2 | Annual-layer results using the StratiCounter program. Maximum-likelihood number of annual layers and confidence intervals derived from annual-layer counting between distinctive marker horizons and corresponding ages relative to the 775 CE ^{10}Be event.

730 *UE: Unattributed volcanic signal and year of sulfate deposition based on final age models (negative
731 numbers are Year BCE).
732 †Year (BCE/CE) calculated from the number of annual layers relative to the fixed age marker in 775
733 CE.
734 ‡Depth has been estimated from the average depth offset between NEEM-2011-S1 and NEEM.
735 §Fixed age marker based on the 10Be maximum annual value.
736 ||Section with 6 m gap in the NEEM 2011-S1 core DRI data (this section is not used for calculating
737 average age).
738 ¶ This section is based on the NEEM field CFA data, since the DRI data does not cover the entire
739 interval.
740 # Section is based on combined data set of DRI and field-measured CFA data. The number of annual
741 layers in this section from manual interpretation by investigator 1 was 383 (±7), and that of
742 investigator 2 was 393 (±8) layers. Most of the difference between the three layer counts was
743 occurring below 480 m (i.e., before 300 BCE), where data gaps were more frequent.
744 ☆Independent age markers used to constrain annual-layer dating in a second iteration to derive the
745 final ice-core age model NS1-2011.
746 **Tephra particles were extracted from the depth range 327.17–327.25 m depth (see
747 Supplementary Data).
748 ††Unattributed volcanic signal that was previously attributed to the historic 79 CE eruption of
749 Vesuvius[64].

750 **Extended Data Table 3 | Historical documentary evidence for key volcanic eruption age markers**
751 **536-939 CE.** A comprehensive list of all sources, including translations and assessment of the
752 confidence placed in each source and its chronological information is given in Supplementary Data.

753 **Extended Data Table 4 | Large volcanic eruptions during the past 2,500 years.** Years with negative
754 numbers are before the Common Era (BCE). Tentative attribution of ice-core signals to historic

volcanic eruptions is based on the Global Volcanism Program volcanic eruption database[93]. Average temperature for the associated cold year is given for the average of Europe and the Arctic[3].

*Total global aerosol forcing was estimated by scaling total sulfate flux from both polar ice sheets to the reconstructed total (i.e., time integrated) aerosol forcing for Tambora 1815[7] (Methods); for high latitude NH eruptions, Greenland fluxes were scaled by a factor of 0.57[6].

† Unattributed volcanic events (UE) and tentative attributions for non-documented historic eruptions (?) are marked.

Extended Data Table 5 | Post-volcanic cooling. Coldest years and decades (1–2000 CE, JJA temperature wrt. 1901–2000) for Europe[3] and years (500 BCE–1250 CE) and decades (500 BCE–2000 CE) with strong growth reduction in the N-Tree composite(wrt. 1000–1099). Ages of the volcanic events from the ice cores reflect the start of volcanic sulfate deposition in Greenland (NS1-2011 timescale) with the largest 40 events indicated in bold letters and tropical eruptions underlined. Years with negative numbers are before the Common Era (BCE).

* Latewood frost ring in bristlecone pines within ±1 year[34]

References

50 Dahl-Jensen, D. *et al.* Eemian interglacial reconstructed from a Greenland folded ice core. *Nature* **493**, 489-494 (2013).

51 McConnell, J. R. Continuous ice-core chemical analyses using inductively Coupled Plasma Mass Spectrometry. *Environ Sci Technol* **36**, 7-11 (2002).

52 McConnell, J. R. & Edwards, R. Coal burning leaves toxic heavy metal legacy in the Arctic. *P Natl Acad Sci USA* **105**, 12140-12144 (2008).

53 Pasteris, D. R. *et al.* Seasonally resolved ice core records from West Antarctica indicate a sea ice source of sea-salt aerosol and a biomass burning source of ammonium. *J Geophys Res-Atmos* **119**, 9168-9182 (2014).

54 Abram, N. J., Mulvaney, R. & Arrowsmith, C. Environmental signals in a highly resolved ice core from James Ross Island, Antarctica. *J Geophys Res-Atmos* **116**, D20116, doi: 10.1029/2011jd016147 (2011).

55 Kaufmann, P. R. *et al.* An Improved Continuous Flow Analysis System for High-Resolution Field Measurements on Ice Cores. *Environ Sci Technol* **42**, 8044-8050 (2008).

56 Bigler, M. *et al.* Optimization of High-Resolution Continuous Flow Analysis for Transient Climate Signals in Ice Cores. *Environ Sci Technol* **45**, 4483-4489 (2011).

57 Ruth, U., Wagenbach, D., Steffensen, J. P. & Bigler, M. Continuous record of microparticle concentration and size distribution in the central Greenland NGRIP ice core during the last glacial period. *J Geophys Res-Atmos* **108**, doi: 10.1029/2002jd002376 (2003).

58 Woodruff, T. E., Welten, K. C., Caffee, M. W. & Nishiizumi, K. Interlaboratory comparison of Be-10 concentrations in two ice cores from Central West Antarctica. *Nucl Instrum Meth B* **294**, 77-80 (2013).

59 Berggren, A. M. *et al.* Variability of Be-10 and delta O-18 in snow pits from Greenland and a surface traverse from Antarctica. *Nucl Instrum Meth B* **294**, 568-572 (2013).

60 Bisiaux, M. M. *et al.* Changes in black carbon deposition to Antarctica from two high-resolution ice core records, 1850-2000 AD. *Atmos Chem Phys* **12**, 4107-4115 (2012).

61 Pasteris, D., McConnell, J. R., Edwards, R., Isaksson, E. & Albert, M. R. Acidity decline in Antarctic ice cores during the Little Ice Age linked to changes in atmospheric nitrate and sea salt concentrations. *J Geophys Res-Atmos* **119**, 5640-5652 (2014).

62 Rasmussen, S. O. *et al.* A first chronology for the North Greenland Eemian Ice Drilling (NEEM) ice core. *Clim Past* **9**, 2713-2730 (2013).

63 Coulter, S. E. *et al.* Holocene tephras highlight complexity of volcanic signals in Greenland ice cores. *J Geophys Res-Atmos* **117**, D21303, doi: 10.1029/2012jd017698 (2012).

64 Barbante, C. *et al.* Greenland ice core evidence of the 79 AD Vesuvius eruption. *Clim Past* **9**, 1221-1232 (2013).

65 Clausen, H. B. *et al.* A comparison of the volcanic records over the past 4000 years from the Greenland Ice Core Project and Dye 3 Greenland Ice Cores. *J Geophys Res-Oceans* **102**, 26707-26723 (1997).

66 Rolandi, G., Paone, A., Di Lascio, M. & Stefani, G. The 79 AD eruption of Somma: The relationship between the date of the eruption and the southeast tephra dispersion. *J Volcanol Geoth Res* **169**, 87-98 (2008).

67 Sun, C. Q. *et al.* Ash from Changbaishan Millennium eruption recorded in Greenland ice: Implications for determining the eruption's timing and impact. *Geophys Res Lett* **41**, 694-701 (2014).

68 Xu, J. D. *et al.* Climatic impact of the Millennium eruption of Changbaishan volcano in China: New insights from high-precision radiocarbon wiggle-match dating. *Geophys Res Lett* **40**, 54-59 (2013).

69 Deirmendjian, D. On volcanic and other particulate turbidity anomalies. *Advances in Geophysics* **16**, 267-296 (1973).

70 Vollmer, M. Effects of absorbing particles on coronas and glories. *Appl Optics* **44**, 5658-5666 (2005).

71 Sachs, A. J. & Hunger, H. Astronomical diaries and related texts from Babylonia. Volume 3: Diaries from 164 B.C. to 61 B.C. Wien: Verlag der Österreichischen Akademie der Wissenschaften (1996).

72 Wittmann, A. D. & Xu, Z. T. A Catalog of Sunspot Observations from 165 Bc to Ad 1684. *Astron Astrophys Sup* **70**, 83-94 (1987).

73 Rasmussen, S. O. *et al.* A new Greenland ice core chronology for the last glacial termination. *J Geophys Res-Atmos* **111**, D06102 doi: 10.1029/2005jd006079 (2006).

74 Herron, M. M., Herron, S. L. & Langway, C. C. Climatic Signal of Ice Melt Features in Southern Greenland. *Nature* **293**, 389-391 (1981).

75 Gao, C. H., Oman, L., Robock, A. & Stenchikov, G. L. Atmospheric volcanic loading derived from bipolar ice cores: Accounting for the spatial distribution of volcanic deposition. *J Geophys Res-Atmos* **112**, D09109, doi: 10.1029/2006jd007461 (2007).

76 Briffa, K. R. *et al.* Trends in recent temperature and radial tree growth spanning 2000 years across northwest Eurasia. *Philos T R Soc B* **363**, 2271-2284 (2008).

77 Grudd, H. Tornetrask tree-ring width and density AD 500-2004: a test of climatic sensitivity and a new 1500-year reconstruction of north Fennoscandian summers. *Clim Dynam* **31**, 843-857 (2008).

78 Salzer, M. W., Bunn, A. G., Graham, N. E. & Hughes, M. K. Five millennia of paleotemperature from tree-rings in the Great Basin, USA. *Clim Dynam* **42**, 1517-1526 (2014).

79 McMahon, S. M., Parker, G. G. & Miller, D. R. Evidence for a recent increase in forest growth. *P Natl Acad Sci USA* **107**, 3611-3615 (2010).

80 Salzer, M. W., Hughes, M. K., Bunn, A. G. & Kipfmueller, K. F. Recent unprecedented tree-ring growth in bristlecone pine at the highest elevations and possible causes. *P Natl Acad Sci USA* **106**, 20348-20353 (2009).

81 Briffa, K. R. *et al.* Reduced sensitivity of recent tree-growth to temperature at high northern latitudes. *Nature* **391**, 678-682 (1998).

82 Rohde, R. *et al.* A New Estimate of the Average Land Surface Temperature Spanning 1753 to 2011. *Geoinfor Geostat: An Overview* **1**, doi: 10.4172/2327-4581.1000101 (2013).

83 Briffa, K. R. *et al.* Reassessing the evidence for tree-growth and inferred temperature change during the Common Era in Yamalia, northwest Siberia. *Quaternary Sci Rev* **72**, 83-107 (2013).

84 Fritts, H. C., Lofgren, G. R. & Gordon, G. A. Variations in Climate since 1602 as Reconstructed from Tree Rings. *Quaternary Res* **12**, 18-46 (1979).

85 Jensen, B. J. L. *et al.* Transatlantic distribution of the Alaskan White River Ash. *Geology* **42**, 875-878 (2014).

86 Oskarsson, N., Sigvaldason, G. E. & Steinthorsson, S. A Dynamic-Model of Rift-Zone Petrogenesis and the Regional Petrology of Iceland. *J Petrol* **23**, 28-74 (1982).

87 Kuehn, S. C., Froese, D. G., Shane, P. A. R. & Participants, I. I. The INTAV intercomparison of electron-beam microanalysis of glass by tephrochronology laboratories: Results and recommendations. *Quatern Int* **246**, 19-47 (2011).

88 Kaufman, D. S. *et al.* Late Quaternary tephrostratigraphy, Ahklun Mountains, SW Alaska. *J Quaternary Sci* **27**, 344-359 (2012).

89 Lakeman, T. R. *et al.* Holocene tephras in lake cores from northern British Columbia, Canada. *Can J Earth Sci* **45**, 935-947 (2008).

90 Bursik, M., Sieh, K. & Meltzner, A. Deposits of the most recent eruption in the Southern Mono Craters, California: Description, interpretation and implications for regional marker tephras. *J Volcanol Geoth Res* **275**, 114-131 (2014).

91 Sampson, D. E. & Cameron, K. L. The Geochemistry of the Inyo Volcanic Chain - Multiple Magma Systems in the Long Valley Region, Eastern California. *J Geophys Res-Solid* **92**, 10403-10421 (1987).

92 Veres, D. *et al.* The Antarctic ice core chronology (AICC2012): an optimized multi-parameter and multi-site dating approach for the last 120 thousand years. *Clim Past* **9**, 1733-1748 (2013).

93 Siebert, L., Simkin, T. & Kimberly, P. *Volcanoes of the World*. 3rd edn, University of California Press (2010).

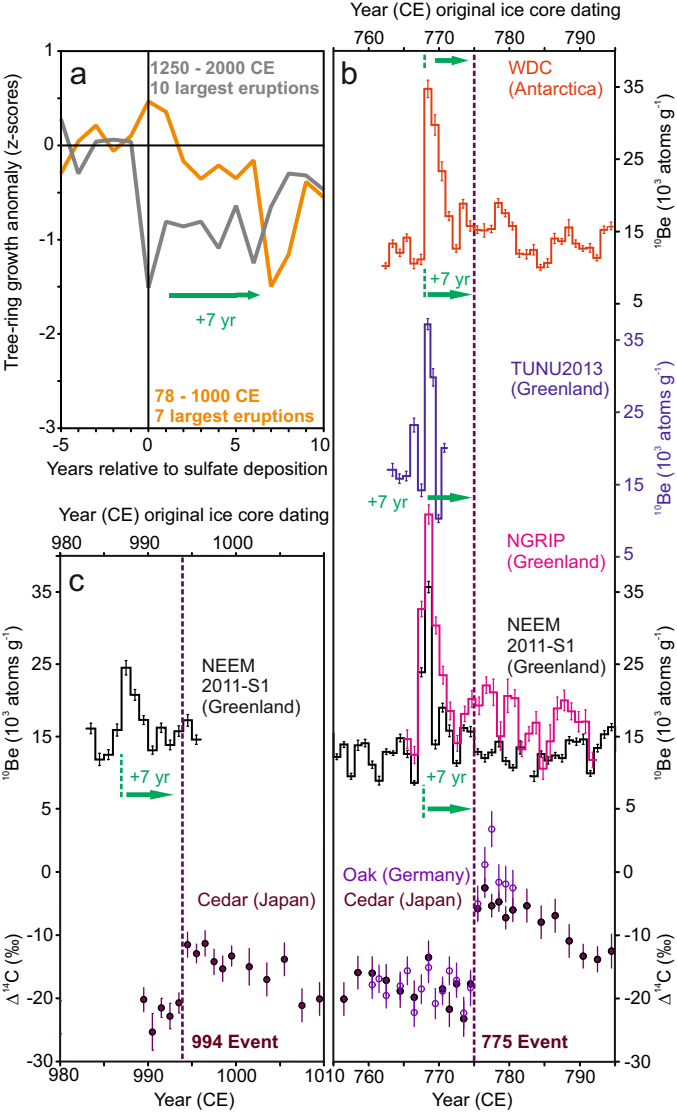
a
1250 - 2000 CE
10 largest eruptions
+7 yr
78 - 1000 CE
7 largest eruptions
Tree-ring growth anomaly (z-scores)
Years relative to sulfate deposition
b
Year (CE) original ice core dating
WDC
(Antarctica)
TUNU2013
(Greenland)
NGRIP
(Greenland)
NEEM
2011-S1
(Greenland)
Oak (Germany)
Cedar (Japan)
775 Event
10Be (10^3 atoms g^-1)
Year (CE)
c
NEEM
2011-S1
(Greenland)
Cedar (Japan)
994 Event
Δ14C (‰)

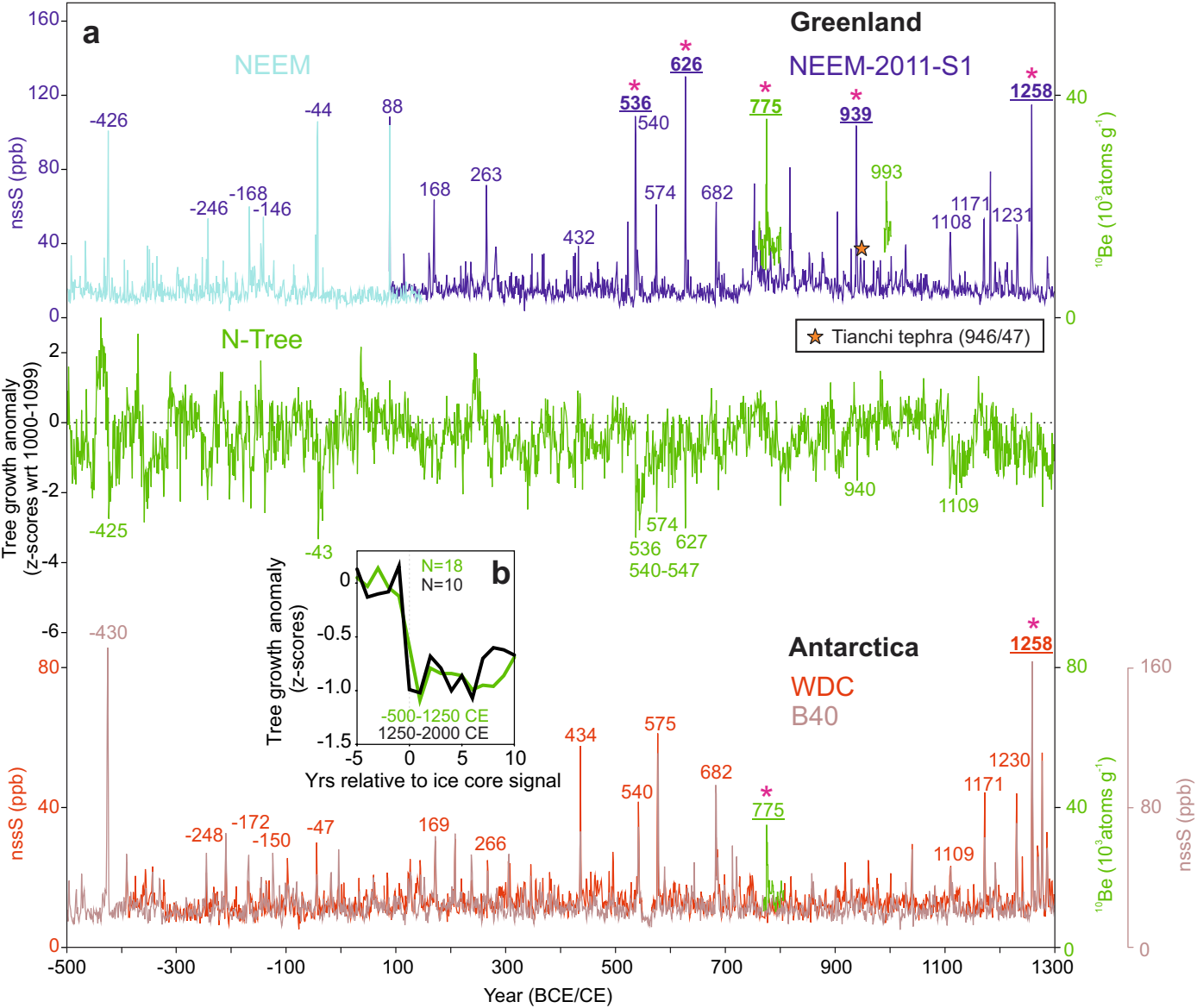
a
Greenland
NEEM
NEEM-2011-S1
nssS (ppb)
^{10}Be (10^3atoms g^{-1})
-426
-246
-168
-146
-44
88
168
263
432
536
540
574
626
682
775
939
993
1108
1171
1231
1258
Tianchi tephra (946/47)
N-Tree
Tree growth anomaly
(z-scores wrt 1000-1099)
-425
-43
536
540-547
574
627
940
1109
b
N=18
N=10
-500-1250 CE
1250-2000 CE
Tree growth anomaly (z-scores)
Yrs relative to ice core signal
Antarctica
WDC
B40
-430
-248
-172
-150
-47
169
266
434
540
575
682
775
1109
1171
1230
1258
nssS (ppb)
^{10}Be (10^3atoms g^{-1})
Year (BCE/CE)

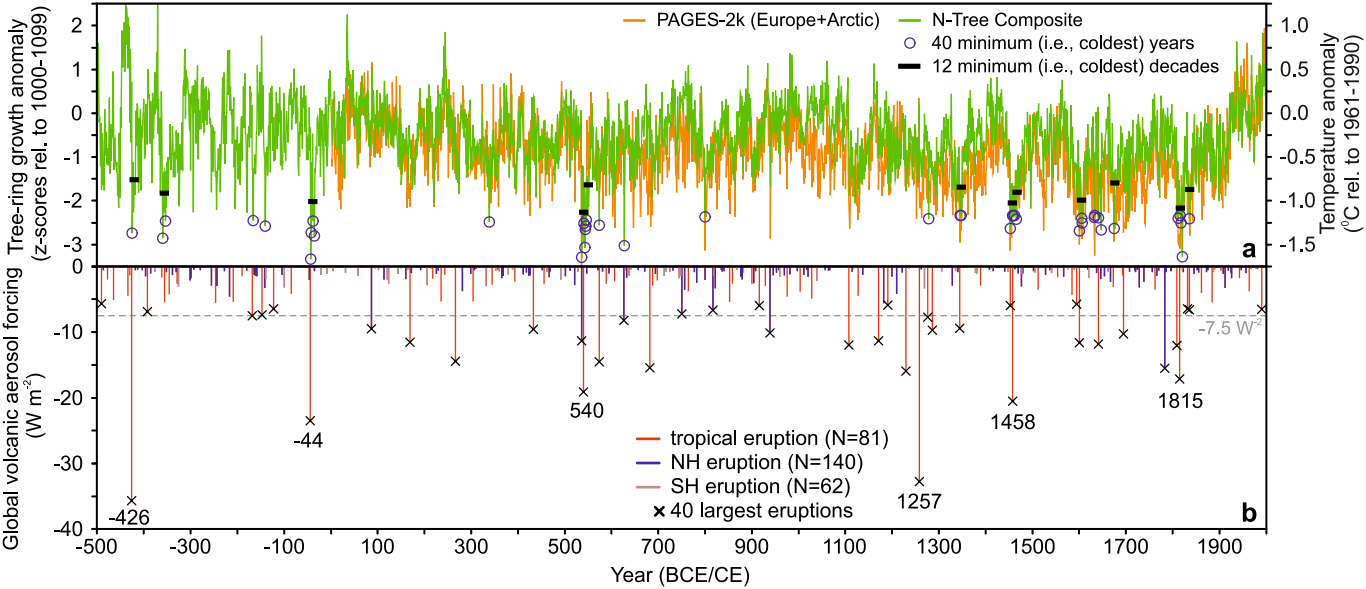
PAGES-2k (Europe+Arctic)
N-Tree Composite
40 minimum (i.e., coldest) years
12 minimum (i.e., coldest) decades
Tree-ring growth anomaly (z-scores rel. to 1000-1099)
Temperature anomaly (°C rel. to 1961-1990)
a
Global volcanic aerosol forcing (W m-2)
-7.5 W-2
-426
-44
540
1257
1458
1815
tropical eruption (N=81)
NH eruption (N=140)
SH eruption (N=62)
40 largest eruptions
b
Year (BCE/CE)

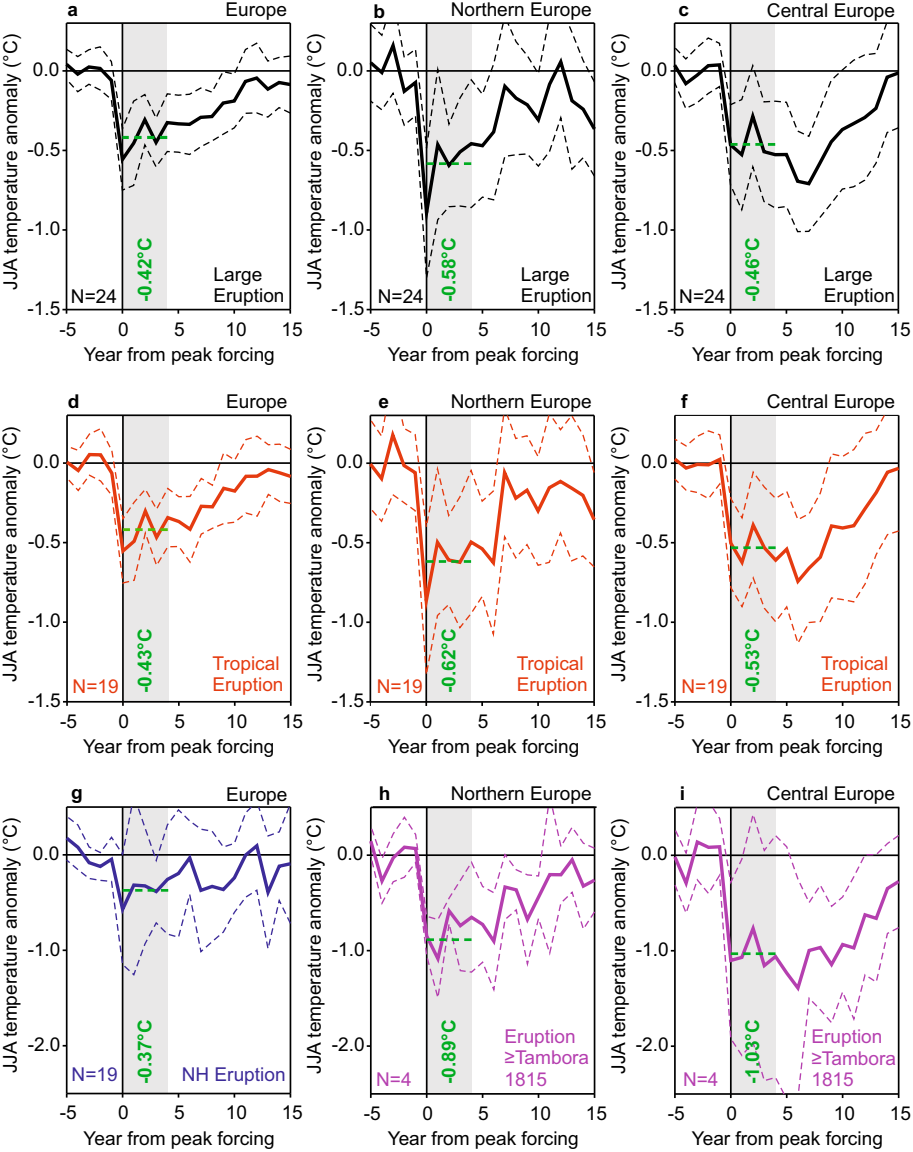
a
Europe
b
Northern Europe
c
Central Europe
JJA temperature anomaly (°C)
0.0
-0.5
-1.0
-1.5
N=24
-0.42°C
Large Eruption
-0.58°C
-0.46°C
-5
0
5
10
15
Year from peak forcing
d
Europe
e
Northern Europe
f
Central Europe
N=19
-0.43°C
Tropical Eruption
-0.62°C
-0.53°C
g
Europe
h
Northern Europe
i
Central Europe
-2.0
-0.37°C
NH Eruption
N=4
-0.89°C
Eruption ≥Tambora 1815
-1.03°C

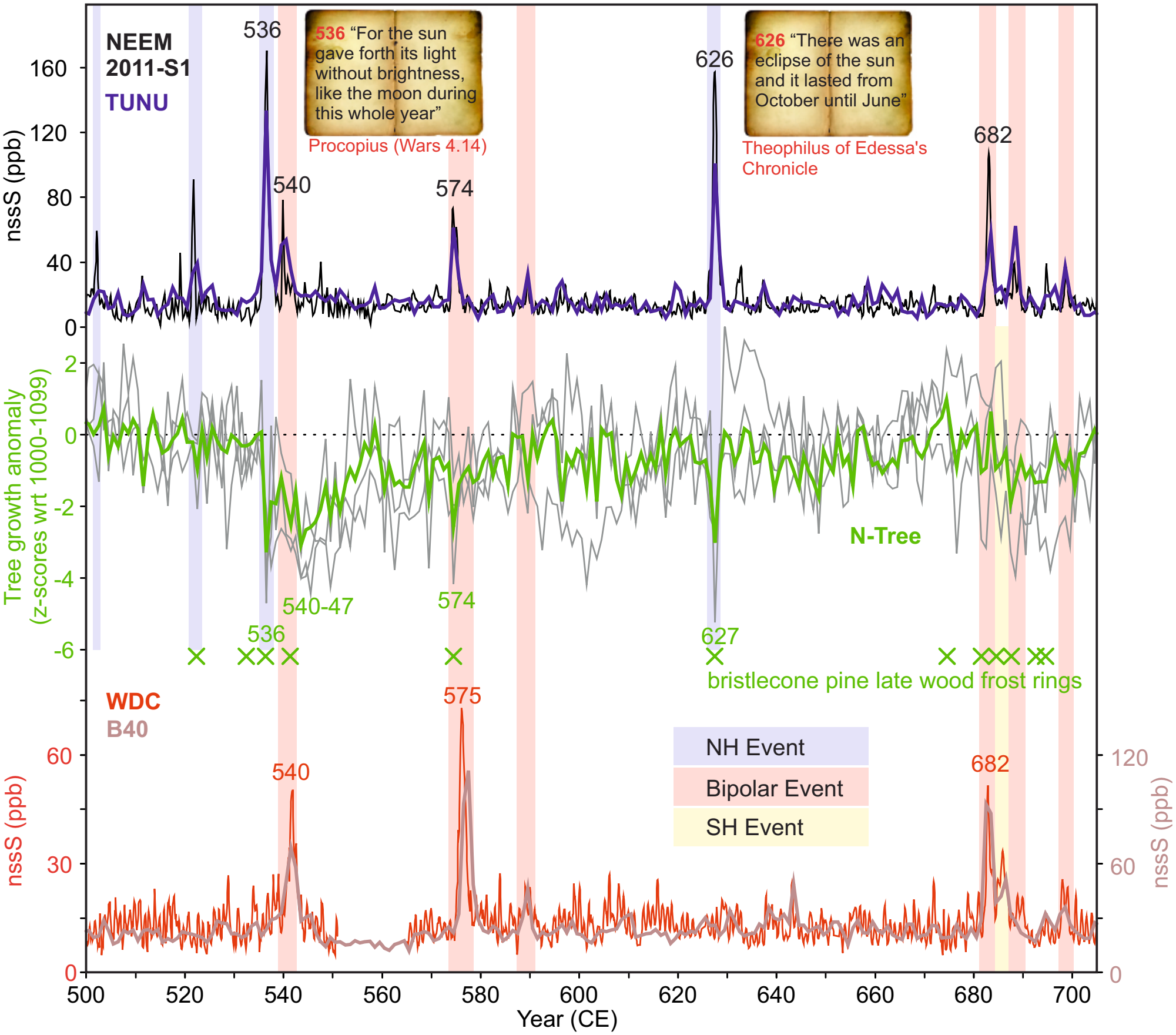
NEEM
2011-S1
TUNU
536
540
574
626
682
536 "For the sun gave forth its light without brightness, like the moon during this whole year"
Procopius (Wars 4.14)
626 "There was an eclipse of the sun and it lasted from October until June"
Theophilus of Edessa's Chronicle
nssS (ppb)
160
120
80
40
0
Tree growth anomaly (z-scores wrt 1000-1099)
2
0
-2
-4
-6
N-Tree
540-47
574
536
627
bristlecone pine late wood frost rings
WDC
B40
575
540
682
NH Event
Bipolar Event
SH Event
60
30
0
120
60
0
500
520
540
560
580
600
620
640
660
680
700
Year (CE)

Extended Data

Timing and climate forcing of volcanic eruptions for the past 2,500 years

M. Sigl[1*], M. Winstrup[2], J.R. McConnell[1], K.C. Welten[3], G. Plunkett[4], F. Ludlow[5], U. Büntgen[6], M. Caffee[7,8], N. Chellman[1], D. Dahl-Jensen[9], H. Fischer[10], S. Kipfstuhl[11], C. Kostick[12], O.J. Maselli[1], F. Mekhaldi[13], R. Mulvaney[14], R. Muscheler[13], D.R. Pasteris[1], J.R. Pilcher[4], M. Salzer[15], S. Schüpbach[10], J.P. Steffensen[9], B.M. Vinther[9], T.E. Woodruff[7]

Find figure captions & footnotes in the main text

Extended Data Figure 1 | Location of study sites.

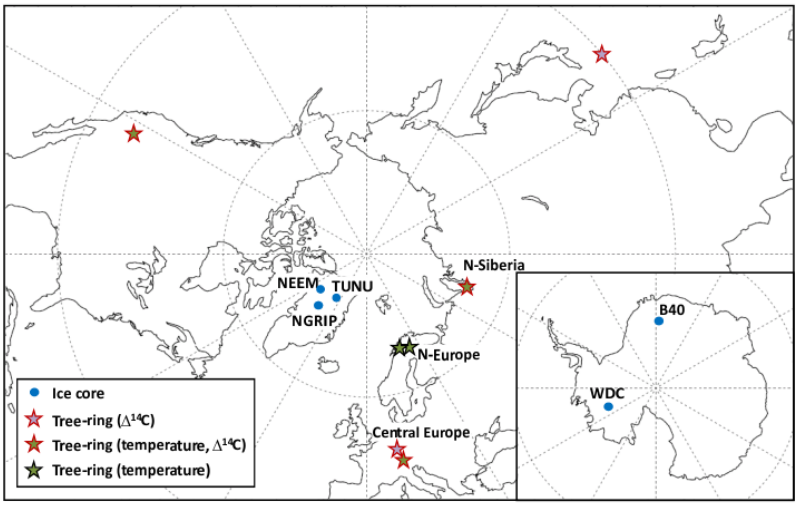

Extended Data Figure 2 | Volcanic dust veils from historical documentary sources in relation to NEEM.

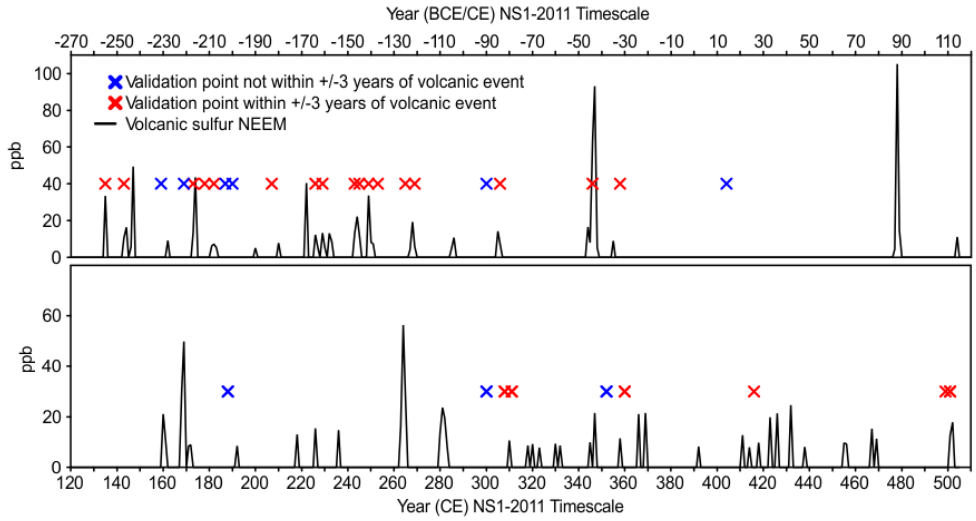

Extended Data Figure 3 | Timescale comparison.

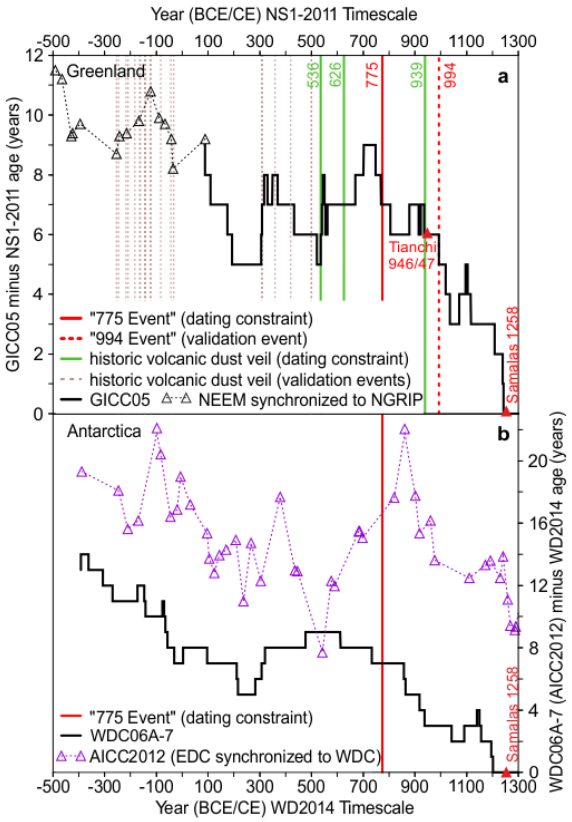

Extended Data Figure 4 | Post-volcanic suppression of tree growth.

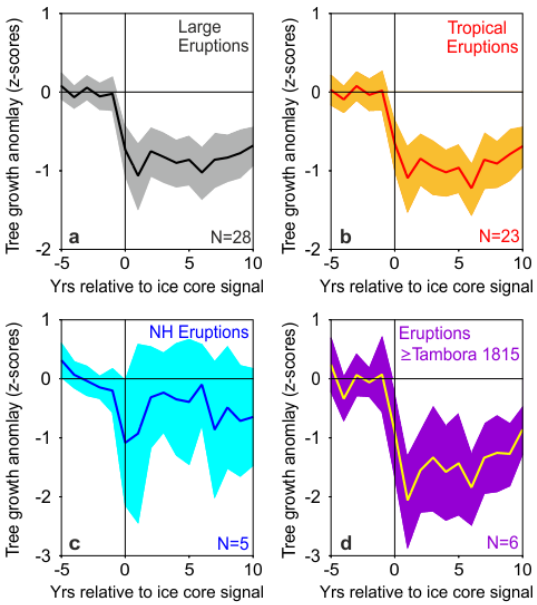

Extended Data Figure 5 | Major element composition for ice core tephra QUB-1859 and reference material.

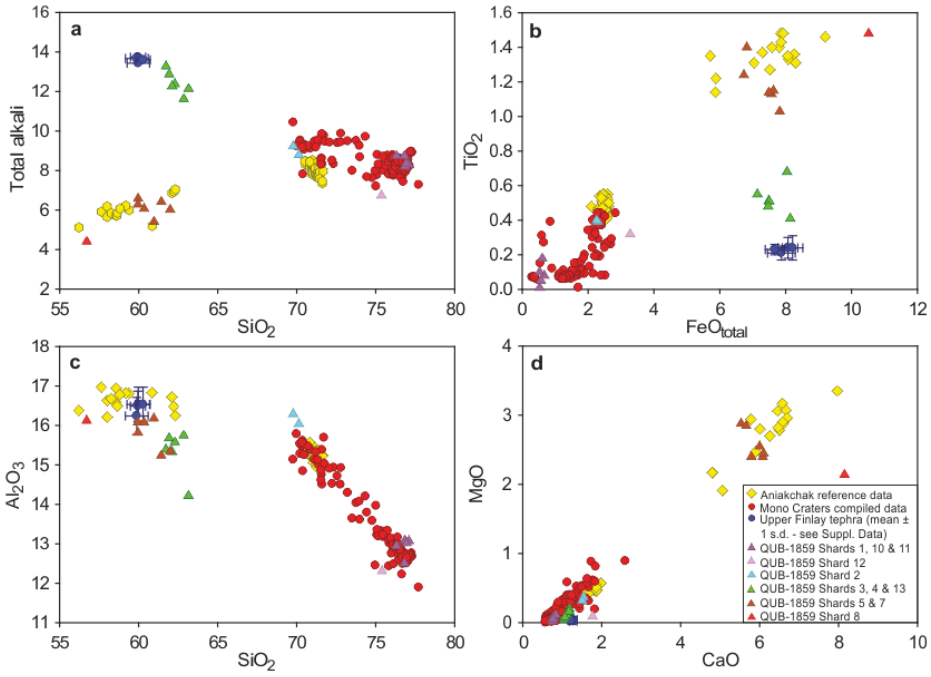

Extended Data Table 1 | Ice-core dating.

Ice Core	Ice-core parameter	Dominant aerosol source	Deposition maximum
NEEM-2011-S1, (Greenland), 183-411m	Na, Cl	sea salt	winter
	nssS, nssS/Na	marine biogenic emissions	summer
	nssCa, Mn, Ce	dust	spring
	BC, NH_4^+, BC geometric mean particle size	biomass burning	summer
	Sr, Mg, I, NO_3^-	various	
NEEM, (Greenland), 183-410m	Na^+	sea salt	winter
	Ca^{2+}, particle count	dust	spring
	NH_4^+, NO_3^-	biomass burning	summer
	conductivity, ECM, H_2O_2	various	
NEEM, (Greenland), 410-514m	Na, Sr, Cl, Na^+	sea salt	winter
	nssS, nssS/Na	marine biogenic emissions	summer
	nssCa, Mn, Mg, particle count, Ca^{2+}	dust	spring
	BC, NH_4^+, NO_3^- ,NH_4^+, NO_3^-	biomass burning	summer
	conductivity, ECM, H_2O_2	various	
WDC, (Antarctica), 188-577m	Na, Sr	sea salt	austral winter
	nssS, nssS/Na, Br	marine biogenic emissions	austral summer
	BC	biomass burning	austral summer/fall

Year CE	Depth (m)	Event	Parameter	Independent age information
NEEM-2011-S1				
1258*	183.49	volcano (tropical)	nssS	ice core (GICC05, Law Dome)
994†	237.89	cosmic ray anomaly	^{10}Be	tree ring
946†	247.21	volcano (NH, Tianchi)	nssS, tephra	historical observation
939*	248.87	volcano (NH, Eldgjá)	nssS	historical observation
775*	281.45	cosmic ray anomaly	^{10}Be	tree ring
626*	310.01	volcano (NH)	nssS	historical observation
536*	327.23	volcano (NH)	nssS, tephra	historical observation
WDC				
1258*	188.91	volcano (tropical)	nssS	ice core (GICC05, Law Dome)
775#	303.36	cosmic ray anomaly	^{10}Be	tree ring

Extended Data Table 2 | Annual-layer results using the StratiCounter program.

Bipolar marker horizons

Event[*]	Depth (m)			Annual layers between horizons [95% confidence interval]				
	WDC	NEEM-2011-S1	NEEM	WDC	NEEM-2011-S1	NEEM	Weighted average [2σ]	Year [2σ][†] (BCE/CE)
Samalas	188.81	183.43	183.05					1259 [±2]
775 Event	303.37	281.25	280.89[‡]	484 [481;487]	482 [479;485]	486 [483;490]	484 [±2]	775[§]
UE 682	326.01	299.26	298.80	92 [91;93]	92 [91;93]	93 [93;95]	92 [±1]	683 [±1]
UE 574	351.67	320.33	319.95	108 [108;108]	109 [108;110]	109 [107;111]	108 [±1]	575 [±2]
UE 540	360.03	326.61	326.25	34 [34;35]	36[‖] [35;37]	33 [33;34]	34 [±1]	541 [±2]
UE 266	423.81	377.43	377.15	274 [272;277]	273 [270;276]	272 [271;274]	273 [±2]	268 [±3]
UE -44	495.21		433.80	312 [310;315]		310 [309;313][¶]	311 [±2]	-44 [±4]
UE -426			501.15			385 [383; 389][#]	385 [±4][#]	-429 [±6][#]

Greenland marker horizons

Event	Depth (m)		Number annual layers [95% confidence]		Maximum likelihood year (wrt to 775 CE)		Independent Age (CE)
	NEEM-2011-S1	NEEM	NEEM-2011-S1	NEEM	NEEM-2011-S1	NEEM	
Samalas	183.43	183.05			1257	1261	1257/58[☆]
Eldgjá	248.76	248.40	317 [315;319]	320 [318;323]	940	941	939[☆]
775 Event	281.25	280.89[‡]	165 [163;167]	166 [164;168]	775[§]	775[§]	775[§]
UE 626/27	309.96	309.60	148 [147;149]	150 [148;152]	627	625	626/627[☆]
UE 536/37[**]	327.20	326.84	92[‖] [91;94]	89 [88;90]	535	536	536[☆]
UE 87/88[††]	410.56	410.20	446 [443;449]	449 [446;452]	89	87	

Extended Data Table 3 | Historical documentary evidence for key volcanic eruption age markers 536-939 CE.

Year (Start)	Summary	Translation	Selected source(s)	Confidence
536	Diminished sunlight for >12 months (Mediterranean)	For the sun gave forth its light without brightness, like the moon, during this whole year, and it seemed exceedingly like the sun in eclipse, for the beams it shed were not clear nor such as it is accustomed to shed.	Procopius, History of the Wars, H.B. Dewing, trans. (Harvard, 1916), 4.14. (five additional sources)	High; Eyewitness or contemporary with a reliable chronology.
626	Diminished sunlight for 9 months (Mediterranean, NW Europe)	There was an eclipse of the sun and it lasted from October [626] until June [627], that is, for nine months. Half of its disc was eclipsed and the other half not; only a little of its light was visible.	Theophilus of Edessa's Chronicle, R.G. Hoyland, trans. (Liverpool, 2011), p. 73. (five additional sources)	High; Eyewitness or contemporary but with some chronological uncertainty.
939	Diminished sunlight (Mediterranean, NW Europe)	We observed the sun: it did not have any strength, brightness, nor heat. Indeed, we saw the sky and its colour changed, as if flushed. And others said that the sun was seen as if halved.	Annales Casinates, Monumenta Germaniae Historica, Scriptores, ed. G.H. Pertz (Hannover, 1839), p. 172. Trans. for this paper by C. Kostick. (three additional sources)	High; Eyewitness or contemporary with a reliable chronology.

Extended Data Table 4 | Large volcanic eruptions during the past 2,500 years.

Rank	Year	Volc. SO_4^{2-} Greenland ($kg\ km^{-2}$)	Volc. SO_4^{2-} Antarctica ($kg\ km^{-2}$)	Global forcing* ($W\ m^{-2}$)	Cold year	N-Tree (z scores; 1000-99)	$T_{Europe/Arctic}$ (^0C; 1961-90)	Volcano†/ Region
1	-426	99.8	78.2	-35.6	-425	-2.74		UE -426
2	1258	90.4	73.4	-32.8	1258	-1.57	-0.91	Samalas/Indonesia
3	-44	100.6	15.4	-23.2	-43	-3.33		Chiltepe?/Nicaragua
4	1458	39.0	63.6	-20.5	1459	-2.35	-1.03	Kuwae/Vanuatu
5	540	61.2	34.4	-19.1	541	-2.52	-1.48	Ilopango?/El Salvador
6	1815	39.7	45.8	-17.1	1816	-2.33	-1.55	Tambora/Indonesia
7	1230	56.4	23.1	-15.9	1230	-1.78	-0.65	UE 1230
8	1783	135.8		-15.5	1783	-0.89	-0.97	Laki/Iceland
9	682	38.4	38.7	-15.4	682	-0.92	-0.96	Pago?/New Britain
10	574	38.3	34.1	-14.5	574	-2.56	-0.94	Rabaul?/New Britain
11	266	61.0	11.3	-14.5	267	-1.25	-0.35	UE 266
12	1809	34.6	25.4	-12.0	1810	-2.32	-1.23	UE 1809
13	1108	48.3	11.6	-12.0	1109	-1.88	-1.15	UE 1108
14	1641	44.2	14.9	-11.8	1641	-2.39	-1.19	Parker/Philippines
15	1601	39.2	18.7	-11.6	1601	-2.68	-1.50	Huaynaputina/Peru
16	169	39.1	18.4	-11.5	170	-0.61	-0.94	UE 169
17	1171	37.0	19.5	-11.3	1171	-0.88	-0.88	UE 1171
18	536	99.0		-11.3	536	-3.29	-1.74	UE 536
19	1695	28.6	22.5	-10.2	1696	-1.79	-1.28	UE 1695
20	939	88.7		-10.1	940	-1.66	-1.44	Eldgjá/Iceland
21	1286	27.6	20.8	-9.7	1288	-1.53	-0.65	Quilotoa?/Ecuador
22	433	20.6	27.2	-9.6	433	0.41	-0.23	UE 433
23	87	83.1		-9.5	87	-0.35	-0.49	UE 87
24	1345	27.9	19.1	-9.4	1346	-2.34	-1.48	El Chichon?/Mexico
25	626	72.2		-8.2	627	-3.02	-0.93	UE 626

Extended Data Table 5 | Post-volcanic cooling.

Rank	Year	JJA temperature anomaly (°C)	Volcanic event(s)	Decade	JJA temperature anomaly (°C)	Volcanic event(s)
1	1821	-1.82	**1815**, 1821	1600-1609	-1.17	1595, **1601**
2	1601	-1.82	**1600**	536-545	-1.12	**536**, **540**
3	1675	-1.78	1673	1812-1821	-1.10	**1809**, **1815**
4	536	-1.67	536	1453-1462	-1.01	**1453**, **1458**
5	800	-1.66	800	1587-1596	-0.98	1585, 1590, **1595**
6	1816	-1.64	**1815**	1107-1116	-0.96	**1108**, 1115
7	1453	-1.57	**1453**	1344-1353	-0.87	1341, **1345**
8	1633	-1.56		351-360	-0.83	351, 358, 360
9	1109	-1.56	**1108**	1692-1701	-0.82	1693, **1695**
10	1608	-1.53		413-422	-0.79	411, 418
11	544	-1.50	**540**	1463-1472	-0.79	**1458**, 1463, 1470
12	574	-1.48	**574**	1127-1136	-0.79	1127
13	1695	-1.47	1693, **1695**	389-398	-0.78	388, 393
14	543	-1.46	**540**	1672-1681	-0.77	1673
15	541	-1.43	**540**	1632-1641	-0.76	1637, **1641**
16	549	-1.43	547	1258-1267	-0.76	**1258**

Rank	Year	Tree growth anomaly (z-scores)	Volcanic event(s)	Decade	Tree growth anomaly (z-scores)	Volcanic event(s)
1	-43*	-3.3	**-44**	536-545	-2.3	**536**, **540**
2	536*	-3.3	**536**	1812-1821	-2.2	**1809**, **1815**
3	543	-3.1	**540**	1453-1462	-2.1	**1453**, **1458**
4	627*	-3.0	**626**	-43 to -34	-2.0	-46, -**44**
5	-360	-2.9	-360	1601-1610	-2.0	**1600**
6	-35	-2.8	-35	-361 to -352	-1.8	-360,-356
7	-425*	-2.7	**-426**	1463-1472	-1.8	**1458**, 1463
8	-42*	-2.7	**-44**	1832-1841	-1.7	**1831**, **1835**
9	544	-2.6	**540**	1344-1353	-1.7	**1344**
10	545	-2.6	**540**	546-555	-1.6	**540**, 547
11	-140*	-2.6	-141	1672-1681	-1.6	1673
12	574*	-2.6	**574**	-425 to -416	-1.5	**-426**
13	541*	-2.5	**540**	1699-1708	-1.5	**1695**, 1708
14	-354*	-2.5	-356	1641-1650	-1.5	**1641**, 1646
15	-38	-2.5		1330-1339	-1.5	1329, 1336
16	-166	-2.4	**-168**	335-344	-1.4	332

Supplementary Data: Historical documentary evidence of volcanism in 79, 536-37, 626-627, 939 CE						
Date	**Source Number**	**Author and/or source**	**Rank †**	**Translation**	**References**	**Notes**
Event 1, Consensus Date, 536-537, Age Marker						
536-537	1	*The Chronicle of Pseudo-Zachariah Rhetor*	A	The whole city was disturbed, and the earth with all that is upon it shook at the arrival of Agapetus [Pope Agapetus I arrived in Constantinople, March 536]. The sun began to become dark at daytime, and the moon by night, while the ocean was stormy with spray [alternatively: clouded by spray] from the 24th of the same month of this year [March, 536] until the 24th of June of the following [indiction] year fifteen [537] … The winter was [so] harsh that from the unusual amount of snow the winged creatures perished, and ... [from here there are lacunae in the manuscript] there was affliction ... that people in ... from awful things and ... not in each place that they were exposed to it.	*The Chronicle of Pseudo-Zachariah Rhetor*, Geoffrey Greatrex, ed., R.R. Phenix & C.B. Horn, trans., (Liverpool, 2011), p. 370.	
Uncertain: 534, 536 or 537	2	*Letter of Magnus Aurelius Cassiodorus Senator to Ambrosius, his Deputy*	B	How strange it is, I ask you, to see the principal star [the Sun], and not its usual brightness; to gaze on the moon, glory of the night, at its full, but shorn of its natural splendour? All of us are still observing, as it were, a blue-coloured sun; we marvel at bodies which cast no mid-day shadow, and at that strength of intensest heat reaching extreme and dull tepidity. And this has not happened in the momentary loss of an eclipse, but has assuredly been going on equally through almost the entire year… Hence it is that, for so long, the rays of the stars have been darkened with an unusual colour; that the harvester dreads the novel cold; that the fruits have hardened with the passage of time; that the grapes are bitter in their old age.	*Selected Variae of Magnus Aurelius Cassiodorus Senator*, S.J.B. Barnish, trans. (Liverpool, 1992), p. 180.	The descriptions of these phenomena are those of an eyewitness, but the letter was not dated and historians have variously estimated its date of composition to 534, 536, or 537.
536-537	3	Procopius, *Wars*	A	And it came about during this year that a most dread portent took place. For the sun gave forth its light without brightness, like the moon, during this whole year, and it seemed exceedingly like the sun in eclipse, for the beams it shed were not clear nor such as it is accustomed to shed. And from the time when this thing happened men were free neither from war nor pestilence nor any other thing leading to death. And it was the time when Justinian was in the tenth year of his reign [1 August 536 – 31 July 537].	Procopius, *History of the Wars*, H.B. Dewing, trans. (Harvard, 1916), 4.14.	

535-536	4	John Lydos, *On Portents*	A	If the sun becomes dim because the air is dense from rising moisture - as happened in the course of the recently passed fourteenth indiction [535/536] for nearly a whole year, when Belisarios held the consular office so that the produce was destroyed because of the bad time - it predicts heavy trouble in Europe. And this we have seen from the events themselves, when many wars broke out in the west and that tyranny was dissolved, while India, and the Persian realm, and whatever dry land lies toward the rising sun, were not troubled at all. And it was not even likely that those regions would be affected by the calamity because it was in Europe that the moisture in question evaporated and gathered into clouds dimming the light of the sun so that it did not come into our sight or pierce this dense substance.	Excerpt from John Lydos, *On Portents*, Antti Arjava trans., 'The Mystery Cloud of 536 CE in the Mediterranean Sources', *Dumbarton Oaks Papers*, 59 (2005), 73 – 94, here p. 80.	This source leaves open (but is not confirmation of) the possibility of volcanic atmospheric effects beginning in 535 CE.
536-537	5	Michael the Syrian	B	In the year 848 [536/537] there was a sign in the sun the like of which had never been seen and reported before in the world. If we had not found it recorded in the majority of proved and credible writings and confirmed by trustworthy people, we would not have recorded it; for it is difficult to conceive. So it is said that the sun became dark and its darkness lasted for one-and-a-half years, that is, eighteen months. Each day it shone for about four hours, and still this light was only a feeble shadow. Everyone declared that the sun would never recover its original light. The fruits did not ripen, and the wine tasted like sour grapes.	Michael the Syrian, *Chronicle*, J.B. Chabot, ed. and trans., 2 (Paris, 1899 – 1910), pp. 220 – 221.	Late twelfth century sources, but reliable transmitter of earlier lost texts.
536-537	6	Bar Hebraeus	B	And in the year eight hundred and forty-eight [AG = 536/537 CE] there was a sign in the sun the like of which had never before appeared. The sun became dark and his darkness lasted for eighteen months. Each day the middle of heaven shone faintly with a shadowy light, and every man decided that [the Sun] would never recover its full light. That year the fruits did not ripen and the wine tasted like urine.	*The Chronography of Bar Hebraeus*, E.A. Wallis Budge, trans., 1 (Oxford, 1932), pp. 74 –75.	Late thirteenth century, but broadly reliable transmitter of lost texts.

Event 2, Consensus Date, 626-627, Age Marker						
626-627	1	Theophilus of Edessa	B	There was an eclipse of the sun and it lasted from October [626] until June [627], that is, for nine months. Half of its disc was eclipsed and the other half not; only a little of its light was visible. There was an eclipse of the sun and stars were visible in the daytime.	*Theophilus of Edessa's Chronicle*, R. G. Hoyland, trans. (Liverpool, 2011), p. 73.	Lost eyewitness source, reconstructed from Agapius of Manbij, *Kitab al-'Unwaiv* [A. A. Vasiliev ed., 'Kitab al-'Unvan, histoire universelle ecrite par Agapius (Mahboub) de Menbidj', Part 2.2, *Patrologia Orientalis*, 8 (1912), 399 -547] and Michael the Syrian [Michael the Syrian, *Chronicle*, J. B. Chabot, ed. and trans., 2 (Paris, 1899 – 1910).] Note, the second sentence of this record likely refers to the solar eclipse of 21 April 627, visible as partial across much of the Middle East, whereas the phenomenon described in the first sentence is clearly too long to be an eclipse. Both phenomena are likely conflated in the source because of their thematic similarity [see Event 3 for similar].
627-628	2	Bar Hebraeus	C	And in the sixth year of the Arabs a portion of the hemisphere of the sun departed, and there was darkness from the month of the First Teshrin [October 627] till the month of Haziran [June 628]. [It lasted so long] that men used to say that the sphere of the sun would never become whole and perfect again. And the *zanta,* that is to say the sickness of the *shar'ata* tumour, broke out in Palestine, and tens of thousands of men died of the disease.	*The Chronography of Bar Hebraeus*, E.A. Wallis Budge, trans., 1 (Oxford, 1932), p. 90.	Late thirteenth century, but broadly reliable transmitter of lost texts. Clearly derived from Theophilus, Bar Hebraeus offers more detail, but a date that is one year in advance of Theophilus.
624	3	*Annales Cambriae A*	C	The sun was obscured.	*Annales Cambriae: a translation of Harleian 3859; PRO E.164/1; Cottonian Domitian, A 1; Exeter Cathedral Library MS. 3514 and MS Exchequer DB Neath, PRO E*, P. M. Remfry, trans. (Castle Studies Research and Publishing, 2007), p. 46	Tenth-century Welsh source containing earlier material. The modern editor, P. M. Remfry, believes the date to be inaccurately transmitted, correcting the manuscript's 624 to 627.

623 (uncorrected AD/CE equivalent supplied by McCarthy (2005) - see Notes)	4	*Annals of Tigernach*	B	A dark year.	*The Annals of Tigernach*, trans. Gearóid Mac Niocaill (Cork, 2010). http://www.ucc.ie/celt/published/T100002A/index.html (Accessed 8 September 2014).	High-medieval Irish source that generally faithfully incorporates earlier eyewitness records, though with chronological errors in the seventh century. We follow Daniel McCarthy's systematic and independently verified corrections to the chronology of Irish annalistic texts, which place this event in 627 CE. [See Daniel McCarthy, 'Chronological synchronisation of the Irish Annals', 4th edition, (2005), www.cs.tcd.ie/misc/kronos/chronology/synchronisms/Edition_4/K_trad/K_synch.htm (accessed 8 September 2014).]
624 (uncorrected manuscript AD/CE year)	5	*Annals of Ulster*	B	A dark year.	*The Annals of Ulster to A.D. 1131*, ed. & trans. Sean Mac Airt and Gearóid Mac Niocaill (Dublin, 1983), p. 113.	Late-fifteenth to early-sixteenth-century Irish compilation of many early sources, including eyewitnesses. Known to be generally reliable in incorporating earlier sources, but with chronological errors for the seventh century. We follow McCarthy's corrections (ibid.) in placing this event in 627 CE.
626 (AD/CE equivalent date supplied by modern editor)	6	*Annals of Inisfallen*	D	Eclipse of the sun.	*The Annals of Inisfallen,* ed. & trans., Sean Mac Airt. (Dublin, 1944), p. 87.	High-medieval Irish source, with frequently unreliable chronology in earlier centuries. This source also often severely abbreviates and amends early material. In the present case, it is highly likely that the scribe has misunderstood the report of a dark year as found in earlier sources (and faithfully preserved in the *Annals of Tigernach* and *Annals of Ulster*), inferring that it describes a solar eclipse, though none were visible in Ireland in 626 or 627.

Event 3, Consensus Date, 939, Age Marker						
938 and/or 939	1	*Annales Casinates*	A	In the twelfth indiction [1 September 938 – 31 August 939], the thirteenth day from the end of July [19 July], day six [Friday], day 29 of the lunar month, the sun was eclipsed from the third hour all the way up to nearly the fifth hour. We observed the sun: it did not have any strength, brightness, nor heat. Indeed, we saw the sky and its colour changed, as if flushed. And others said that the sun was seen as if halved.	*Annales Casinates*, Monumenta Germaniae Historica, Scriptores, ed. G.H. Pertz 3 (Hannover, 1839), p. 172. Trans. for this paper by Conor Kostick.	This entry was mistakenly listed under 938 in the manuscript, but the cited indiction year (i.e. the 12th indiction) is correct for September 938 to August 939. The eclipse details as given in the first sentence are precise for the solar eclipse as visible from Monte Cassino, Italy, on 19 July 939. It is not certain whether the second sentence represents a continued description of the solar eclipse, or whether it is a different phenomenon that has been conflated because of its thematic similarity to the eclipse. It possesses many hallmarks of a volcanic dust-veil (e.g. the sun's lack of strength and heat, and a reddened sky). Alternatively, the colourful description may reflect the spectacle of a deep eclipse further enhanced by atmospheric volcanic aerosols.
939	2	*Chronicon Scotorum*	B	The sun was the colour of blood from the beginning of day to midday on the following day.	*Chronicon Scotorum*, William M. Hennessy & Gearóid Mac Niocaill, ed. & trans. (Cork, 2010). http://www.ucc.ie/celt/published/T100016/index.html (Accessed 8 September 2014)	Seventeenth-century Irish source, but with unique content from earlier and now-lost sources. This event, too extended to be a solar eclipse, has been widely considered an observation of Eldgjá's (Iceland) volcanic plume or dust-veil, and is reliably dated to 939. [See Francis Ludlow *et al.*, 'Medieval Irish chronicles reveal persistent volcanic forcing of severe winter cold events, 431-1649 CE', *Environmental Research Letters*, 8 (2013), doi:10.1088/1748-9326/8/2/024035, and references therein.]

933	3	*Mageoghagan's Book*, or *Annals of Clonmacnoise*	C	The sun for one day appeared like blood until noon the next day.	*The Annals of Clonmacnoise, being Annals of Ireland from the earliest period to A.D. 1408, translated into English A.D. 1627 by Conell Mageoghagan and now for the first time printed*, Dennis Murphy, ed. (Dublin, 1896).	Seventeenth-century Irish source that often amends and elaborates upon the content of earlier sources from which it draws. R. B. Stothers ['Far Reach of the Tenth Century Eldgjá Eruption, Iceland', *Climatic Change*, 39 (1998), 715 – 726] uses the 933 date from this source in support of an earlier eruption date for Eldgjá. However, the source has an unreliable chronology for the first millennium CE, and can be shown to have a systematic off-set of 6 years at this time. [See Daniel McCarthy, 'Irish chronicles and their chronology', (2005). www.cs.tcd.ie/misc/kronos/chronology/synchronisms/annals-chron.htm (Accessed 8 September 2014).] Stothers does not note the later and reliable date of 939 (above) from the *Chronicon Scotorum*.

Uncertain: Before July 936, if read verbatim.	4	Widukind of Corvey, *The Deeds of the Saxons*	B	In this year, [941] certain portents appeared, namely comets. For they could be seen from the fifteenth Kalends of November [18 October] all the way up to the Kalends themselves [1 November]. Many people were terrified by these sights, they were dreading either a great pestilence or at any rate a change in royal power. For certain portents were revealed before the passing of King Henry [Henry I, the Fowler, 2 July 936], such as that while outside even though no cloudy tail covered it, the brilliance of the sun failed to appear but inside, that a red colour like blood poured through the windows of houses. The mount also, where the remains of the lord of things [Possibly Úlfljótr, the founder, lawgiver, and first lawspeaker of the united Icelandic Parliament, see R.B. Stothers, 'Far Reach of the Tenth Century Eldgjá Eruption, Iceland', *Climatic Change*, 39 (1998), 715 – 726, here p. 719] are buried, according to rumour, vomited many flames in that region. Furthermore, the left hand of a certain man having been cut off by the sword, almost a year later it was completely restored as he was sleeping, as a sign of this miracle a bloody line was noted at the place of the join. But there were comets and a great flood, and a cattle pestilence followed the flood.	Widukind of Corvey, *The Deeds of the Saxons*, Monumenta Germaniae Historica, Scriptores, ed. G.H. Pertz 3 (Hannover, 1839), II.32. Trans. for this paper by Conor Kostick.	R. B. Stothers [ibid.] argues that the dim sun occurs before 936, also drawing for support upon ice core dates that place an eruption in the early 930s. But doubt exists regarding Widukind's dating of this event, because it clearly suits his purpose to make a failing sun (and other ominous phenomena) act as a portent of the death of King Henry I.
Miscellaneous, 79 CE, Age Marker for GICC05 Chronology						
79	1	Cassius Dio, *Roman History*	B	An inconceivable quantity of ashes was blown out, which covered both sea and land and filled all the air. It wrought much injury of various kinds, as chance befell, to men and farms and cattle, and in particular it destroyed all fish and birds. Furthermore, it buried two entire cities, Herculaneum and Pompeii, the latter place while its populace was seated in the theatre. Indeed, the amount of dust, taken all together, was so great that some of it reached Africa and Syria and Egypt, and it also reached Rome, filling the air overhead and darkening the sun.	Greek text at Marie-Laure Freyburger-Galland, 'Les phénomènes volcaniques chez Dion Cassius' in Eric Foulon, ed. *Connaissance et représentations des volcans dans l'antiquité: actes du colloque de Clermont-Ferrand 2002* (Clermont-Ferrand, 2004), pp. 139 – 157, here p. 144. English translation at http://penelope.uchicago.edu/Thayer/E/Roman/Texts/Cassius_Dio/66*.html (Accessed 25 August 2014).	This historical observation is cited as evidence of a significant southeasterly component in ash dispersal of the 79 CE eruption. [See also G. Rolandi *et al*., 'The 79 AD eruption of Somma: The relationship between the date of the eruption and the southeast tephra dispersion', *Journal of Volcanology and Geothermal Research*, 169 (2007), 87-98.] Note also: The relevant books of Cassius Dio, (66, 21, 1-24, 3) are only available through an epitome, that by the Byzantine monk Joannes Xiphilinus, Constantinople, c. 1075.

† *Source reliability ranking*	*Rationale*
A	Eyewitness or contemporary with a reliable chronology.
B	Eyewitness or contemporary but with some chronological uncertainty. Or: Neither eyewitness nor contemporary but has a reliable chronology and/or accurately conveys the information from earlier works.
C	Eyewitness or contemporary but with evidence of errors or fabrications. Or: Neither eyewitness nor contemporary and with an unreliable chronology.
D	Neither eyewitness nor contemporary and with evidence of errors or fabrication.

Supplementary Data. Historical documentary evidence of volcanic dust veils, pre-536 CE

Date (BCE/CE)	*Summary*	*Rank*	*Sources and/or authors*	*Regions*	*References*
255 BCE	Disk of the sun resembles moon	Probable	Astronomical dairies	Babylonia	Sachs & Hunger (1989)
247	Disk of the sun resembles moon, also multiple incidence of haze and mist, and dense mist [1]	*Possible*	Astronomical dairies	Babylonia	Sachs & Hunger (1989)
231	Disk of the sun resembles moon, multiple observations	Probable	Astronomical dairies	Babylonia	Sachs & Hunger (1989)
221	Disk of the sun resembles moon	Probable	Astronomical dairies	Babylonia	Sachs & Hunger (1989)
217	Sun's disk contracted/diminished; additionally: the sun fights/struggles with the moon [2]	*Possible*	Livy 22.1.9-10	Mediterranean	Stothers (2002)
212	Sun's disk unusually red, like the color of blood	Probable	Livy 25.7.8	Mediterranean	Stothers (2002)
208	Stars fade/invisible for three months	Probable	*Table of dynastic records* (cf. Pang, 1991)	North China	Pang *et al.* (1987), Stothers (2002)
203	Disk of the sun resembles moon; also, mist and haze cover sky, and solar halo	Probable	Astronomical dairies	Babylonia	Sachs & Hunger (1989)
200	Sun's disk appears reddened	Probable	Livy 31.12.5	Mediterranean	Stothers (2002)
183	Disk of the sun resembles moon	Probable	Astronomical dairies	Babylonia	Sachs & Hunger (1989)
164	Disk of the sun resembles moon; also "billowing" solar and lunar halos, and multiple (non-billowing) solar halos	Probable	Astronomical dairies	Babylonia	Sachs & Hunger (1996)
161	Disk of the sun resembles moon	Probable	Astronomical dairies	Babylonia	Sachs & Hunger (1996)
147	Coloured rings surround sun	Probable	Obsequens	Mediterranean	Schlesinger (1959)
145 to 144	Recurring redness over eastern and western skies, September to October [145 BCE]; later, billowing halo (solar/lunar) and further solar and lunar halos [all in 145 BCE]. Reddened skies over Babylon, July to August [144 BCE]	Probable	Astronomical diaries	Babylonia	Stothers (2002), Sachs & Hunger (1996)
141	Disk of the sun resembles moon, multiple observations; also, multiple incidence of billowing solar and lunar halos	Probable	Astronomical dairies	Babylonia	Sachs & Hunger (1996)
137	Disk of the sun resembles moon, multiple observations; also, haze, multiple observations, and solar halo	Probable	Astronomical dairies	Babylonia	Sachs & Hunger (1996)
125 to 124	Billowing solar halo, also multiple billowing lunar halos, and lunar halo, dense haze and mist [3]	*Possible*	Astronomical dairies	Babylonia	Sachs & Hunger (1996)
121	A sky bow surrounds the Sun	*Possible* [4]	Pliny the Elder 2.29 [5]	Mediterranean	Stothers (2002)
90	A red ring surrounds the Sun	Probable	Pliny the Elder 2.29 [5]	Mediterranean	Stothers (2002)
84	Repeated incidence of dense haze & mist [6]	*Possible*	Astronomical dairies	Babylonia	Sachs & Hunger (1996)

44 to 42	Prolongued eclipse of the Sun, almost a year's continuous gloom (Mediterranean); Pale blue sun, casting no shadows (China)	Probable	Mediterranean summary from Pliny the Elder 2.30 [7]; Chinese summary from Han-Shu	Mediterranean, China	Forsyth (1988), Yau *et al.* (1988), Bicknell (1993), Stothers (2002); Oppenheimer (2011)
32	Orange sky, darkness in daytime	Probable	Han-Shu	China	Yau *et al.* (1988)
14 CE	Sun was completely eclipsed [8]	*Possible*	Cassius Dio 56.29.3 & others (see Stothers (2002))	Mediterranean	Stothers (2002)
188	Orange (reddish-yellow) solar disk	Probable	Hou-Han-Shu, Zhi	China	Yau *et al.* (1988)
300	Yellow fog covers the Sun [9]	*Possible*	Song Shu Wu Xing Zhi	China	Wittman & Xu (1987)
308	Sun concealed by dark yellow vapour	Probable	Jin-Shu, Zhi	China	Wittman & Xu (1987)
311	Sunlight discolored red and also anything it illuminates	Probable	Jin-Shu, Zhi	China	Yau *et al.* (1988)
352	Solar disk discolored red	Probable	Chin-Shu	China	Yau *et al.* (1988)
360	Dark mist obscures sky, sun disappears from dawn to noon [10]	*Possible*	Ammianus Marcellinus 20.3.1	Mediterranean or Middle East	McCormick *et al.* (2012)
416 and/or 417	Darkness during the day [11]	Probable	Marcellinus Comes	Mediterranean	Croke (1995), McCormick *et al.* (2012)
499	Sun dispossessed of light at dawn, disk like silver, without brilliance, can be gazed on without harm; phenomenon continues to eighth hour [12]	Probable	Summary from *Chronicle of Pseudo-Joshua Stylite*	Mediterranean	Witakowski (1996), Tombley & Watt (2000), McCormick *et al.* (2012)
501	Sun red and dim, or without brilliance	Probable	Wei-Shu	North China	Wittman & Xu (1987), Yau *et al.* (1988)

NOTES

[1] The relatively rare reports that characterize (in Babylonian astronomical diaries) the disk of the sun as resembling that of the moon, indicating diminished light and a discolored solar disk, are generally taken as probable indications of high-altitude dust or aerosol layers. In this year, 247 BCE, it is also reported that red sand fell from the sky. High-altitude non-volcanic dust may explain (or have additionally contributed to) the rare characterization of the sun this year. We thus rank a volcanic dust-veil this year as Possible, rather than Probable (see Supplementary Methods).

[2] Uncertainty exists over whether this event can be explained by a partial solar eclipse on 11 February 217 BCE, visible widely in the Mediterranean region (Stothers, 2002). While Livy's description of the sun struggling with the moon is reminiscent of a solar eclipse, Livy in fact reports this separately to his description of a diminished sun (a point not noted by Stothers (2002)), and which is more reminiscent of a volcanic dust veil. Given that both events may well be distinct, we include the latter in our list, but assign it a rank of Possible, only.

[3] Solar halos are common in Babylonian astronomical diaries. While some may in fact be volcanic solar coronae (i.e. Bishop's Rings), their description in the diaries rarely allows discrimination. By contrast, solar haloes described as "billowing" are less common. With a notable confluence of additional halos, "dense" haze and mist this year, we consider this sufficient evidence for increased atmospheric turbidity consistent with volcanic atmospheric aerosol presence, meriting inclusion in our list with a rank of Possible, spanning 125 to 124 BCE.

[4] We rank this "sky bow" as Possible because the lack a reference to the colour of the bow leaves open the possibility that it may be a solar halo rather than corona.

[5] Stothers (2002) cites these observations (at 121 and 90 BCE) as found in Book 2, Chapter 98 of Pliny the Elder's *Historia Naturalis*. However, both are correctly found in Book 2, Chapter 29 (i.e. Pliny 2.29).

[6] Haze and mist are often reported in Babylonian astronomical diaries, which is expected given the frequent aridity of the region (present-day Iraq). Thus, such reports do not alone merit inclusion as a validation point. However, for this year (84 BCE) haze and mist (often specifically characterized as "dense") are exceptionally persistent. We take this as indicative of a dry fog or dust-veil, but rank it Possible only.

[7] An extensive literature is available on this dust veil, which is likely to have lasted from 44 to 42 BCE. See literature cited in References column, above.

[8] As Stothers (2002) notes, there is no total solar eclipse for 14 CE in the presumed Mediterranean region of recording that can explain this observation. However, as Stother's further notes, this event may be an allegorical omen of August Caesar's death this year. The event's fabrication cannot be proven, however, and should not be simply assumed. We thus include this event but rank it Possible, only.
[9] This event's description is not fully certain. Wittman & Xu (1987) translate it as: "There was a Sun's fighting, and yellow fog covered all around". The sun's fighting may refer to an eclipse or sunspot, which can be more easily observed when the sun is veiled by high-altitude dust or aerosol and are thus often associated with volcanic dust-veils (Scuderi, 1990). The reference to yellow fog is also notable. We rank this event as Possible.
[10] No solar eclipse occurred for 360 CE in the Mediterranean region. An eclipse occurred further east, visible from central present-day Iraq and eastward into the Pacific (Espenak & Meeus, 2006). Because Ammianus Marcellinus, a major Roman historian, is unlikely to have witnessed this eclipse himself, and because of the incompatibility of many aspects of Ammianus's description with a solar eclipse, the event has generated considerable debate. Scholars have advanced theories concerning communication networks available to Ammianus, his location at the date of the eclipse, and the historical reliability of his reporting (see, e.g., Barnes (1998) and references therein). Few appear to have considered that this report may incorporate genuine aspects of a volcanic dust-veil observation, consistent with much of the description. We thus include the event, ranked Possible.
[11] Marcellinus simply reports that "there was darkness during the day". This stands in marked contrast to his explicit and verifiably correct (see Espenak & Meeus (2006)) report of a solar eclipse occurring in 418 CE, thereby leaving open the nature and duration of the phenomena described here. Moreover, no appropriate eclipse was visible in 416 or 417 CE (Espenak & Meeus, 2006). The exact Julian year date is uncertain because Marcellinus dates according to the Indiction, i.e. the event is dated to the "15th indiction, consulship of Honorius (11th) and Constantius (2nd)", spanning 1 September 416 to 31 August 417 CE (see Croke (1995)). We rank this candidate dust-veil as Probable.
[12] This phenomenon bears many hallmarks of a volcanic dust-veil observation, also occurring for too long to be a solar eclipse. It is reported in several sources (see literature in References column, and citations therein), though with slightly divergent dating. We rank this event a Probable dust-veil, and prefer the date of 499 from Pseudo-Joshua the Stylite (Trombley & Watt, 2000), in being a broadly reliable and probable eye-witness to events at this time.

REFERENCES

Barnes, T. D. (1998) *Ammianus Marcellinus and the representation of historical reality* (New York: Cornell University Press).

Bicknell, P. (1990) Blue Suns, the Son of Heaven, and the chronology of the volcanic veil of the 40s B.C., *The Ancient History Bulletin*, 7 (1), 2-11.

Croke, B. (ed.) (1995) *The Chronicle of Marcellinus: A Translation and Commentary*. Sydney: Australian Association for Byzantine Studies.

Espenak, F. and Meeus, J. (2006) *Five millennium canon of solar eclipses: -1999 to +3000 (2000 BCE to 3000 CE)* (Maryland: NASA).

Forsyth, P. Y. (1988) In the wake of Etna, 44 B.C., *Classical Antiquity*, 7 (1), 49-57.

McCormick, M., Büntgen, U., Cane, M., Cook, E. R., Harper, K., Huybers, P., Litt, T., Manning, S. W., Mayewski, P. A., More, A. M., Nicolussi, K. and Tegel, W. (2012) Climate change during and after the Roman Empire: Reconstructing the past from scientific and historical evidence, *Journal of Interdisciplinary History*, 43 (2), 169-220. doi:10.1162/JINH_a_00379

Oppenheimer, C. (2011) *Eruptions that shook the world*. Cambridge: Cambridge University Press.

Pang. K. D., Slavin, J. A. and Chou, H.-H. (1987) Climatic anomalies of late third century BC: Correlation with volcanism, solar activity, and planetary alignment, *Eos Transactions*, *American Geophysical Union*, 68, 1234.

Pang, K. D. (1991) The legacies of eruption: Matching traces of ancient volcanism with chronicles of cold and famine, *The Sciences*, 31 (1), 30-35.

Sachs, A. J. and Hunger, H. (eds.) (1989) *Astronomical diaries and related texts from Babylonia. Volume 2: Diaries from 261*

B.C. to 165 B.C. Wien: Verlag der Österreichischen Akademie der Wissenschaften.

Sachs, A. J. and Hunger, H. (eds.) (1996) *Astronomical diaries and related texts from Babylonia. Volume 3: Diaries from 164 B.C. to 61 B.C.* Wien: Verlag der Österreichischen Akademie der Wissenschaften.

Schlesinger, A. C. (1959) *Livy Vol. XIV: Summaries, fragments and Obsequens.* Cambridge: Harvard University Press.

Scuderi, L. A. (1990) Oriental sunspot observations and volcanism, *Quarterly Journal of the Royal Astronomical Society*, 31, 109-120.

Stothers, R. B. (2002) Cloudy and clear stratospheres before A.D. 1000 inferred from written sources, *Journal of Geophysical Research*, 107, D23 (4718), doi:10.1029/2002JD002105.

Trombley, F. R. & Watt, J. W. (eds.) (2000) *The chronicle of Pseudo-Joshua the Stylite*. Liverpool: Liverpool University Press.

Witakowski, W. (ed.) (1996) *Pseudo-Dionysus of Tel-Mahre*, *chronicle, part III*. Liverpool: Liverpool University Press.

Wittman, A. D. and Xu, Z. T. (1987) A catalogue of sunspot observations from 165 BC to AD 1684, *Astronomy & Astrophysics Supplement Series*, 70: 83-94.

Yau, K. K. C. and Stephenson, F. R. (1988) A revised catalogue of Far Eastern observations of sunspots (165 BC to AD 1918), *Quarterly Journal of the Royal Astronomical Society*, 29, 175-197.

Supplementary Data: Monte Carlo equal means test of association between NEEM volcanic events and historical validation points

Validation points and probably-only subset	*Margin (years)*	*Validation points with NEEM volcanic events within margin*	*Mean number of NEEM volcanic events observed within each margin (whole period mean, 258 BCE to 504 CE, is 0.11155)*	*Probability of observed value occurring randomly*
All 32 validation points	+/-3	24 of 32 (75.0%)	0.24017 (n = 229, i.e. sum of years in margins)	<0.001
All 32 validation points	+/-2	20 of 32 (62.5%)	0.26061 (n = 165)	<0.001
All 32 validation points	+/-1	16 of 32 (50.0%)	0.30693 (n = 101)	<0.001
24 probable points only	+/-3	18 of 24 (75.0%)	0.21935 (n = 155)	<0.001
24 probable points only	+/-2	14 of 24 (58.3%)	0.25000 (n = 124)	<0.001
24 probable points only	+/-1	11 of 24 (45.8%)	0.28947 (n = 76)	<0.001

Note: We employed a Monte Carlo equal means test (1,000,000 iterations) to compare the number of NEEM volcanic event years on the NS1-2011 timescale that occurred near to our historical validation points (i.e., within each uncertainty margin) to the number that would be expected randomly. We calculated probabilities based upon the number of volcanic event years observed in the period 258 BCE to 504 CE, matching the period covered by our validation points (earliest and latest at 255 BCE and 501 CE), with an additional three years on each side. For reference, the mean number of volcanic event years from 255 BCE to 504 CE (inclusive) is 0.11155. Note that consistent results are obtained when employing an alternative Mann-Whitney (Rank Sum) test (i.e., comparing medians rather than means) in both standard and Monte Carlo implementations.

Response to Referees

First, we would like to thank the referees for their support of our manuscript and their constructive comments. Following is a point-by-point response to the critical comments and recommendations of the referees. Please note that the referees' comments are in black and our response is in blue. Further, we have modified the main text of the manuscript to be consistent with these responses.

Referee #1 (Remarks to the Author):

In this study, the authors present a new, extended estimate of volcanic forcing from Greenland and Antarctic ice cores that spans the last 2,500 years. The authors present a new set of high-resolution Be-10 measurements and use these data to argue that the previous age model for these records was misdated by 7 years during the first millennium CE. By comparing their Be-10 measurements against a pair of C-14 markers identified in tree rings, the authors propose a new age model for these ice cores and use this new sequence to update the long-term record of volcanic emissions for both hemispheres.

I would like the authors to be more precise with some of their statements and interpretations, but overall I found the papers conclusions to be well-supported by their evidence.

Because ice core records provide our only means to understand how large eruptions influence the global climate, the proposed revision of the global volcanic aerosol forcing would be extremely relevant to researchers working in the climate sciences. Because of the significant impact that large eruptions have on human society, I would imagine that archeologists and historians would also regard this as a major contribution.

In addition to the specific comments I include below, I would strongly encourage the authors to consider addressing two issues. First, I would like them to outline, at least briefly, what may have caused the 7-year error in the previous age model. Does this offset imply that, previously, single-year accumulation layers were incorrectly identified as multiple years? Is it possible that there are unconformities in the ice? Could the accumulation rates have been poorly estimated? As a non-expert in this field, I can only guess what factors might have caused this error, but I would hope that they could at least lead their readers to one or more plausible explanations.

The causes of bias in the previous age models likely are due to several factors and would need to be addressed in detail for each ice-core chronology separately. In summary, the offset is due to the combined effects of the following:

1) Low effective resolution of some the ice-core measurements, i.e. low sampling resolution, diffusion (this is especially true for the relevant sections of the GRIP and NGRIP cores where diffusion correction techniques were employed to recover the annual oscillations in water isotope data. This technique is vulnerable to melt layer interference).
2) Use of only single (or a few) parameters for the annual-layer interpretation.
3) Occurrence of intra-annual variations in various ice core parameters falsely interpreted as layer boundaries (e.g., caused by summer melt, dust deposition)
4) Use of tephra believed from the AD 79 Vesuvian eruption as a fixed reference horizon to constrain the Greenland ice-core dating. This attribution seemingly confirmed the Greenland ice core chronologies for the past 2,000 years, thus encouraging glaciologists to focus their

subsequent attention and high-resolution measurement efforts on deeper sections of the GRIP and NGRIP ice cores.

5) Use of manual-layer interpretation techniques that favor annual-layer interpretation consistent with a priori knowledge or existing chronologies (e.g., WDC).

To overcome previous limitations and achieve consistency with proxy records independent of the ice-core records during the Common Era, we employed new and existing high-resolution, multi-parameter ice-core measurements constrained by distinct and well-dated reference horizons and employed an objective algorithm to avoid biasing our interpretation by a priori assumptions.

We summarized some plausible explanations and added citations in methods.

Second, I worry that some readers might interpret this evidence very differently. The authors explain that, with the original dating, there is a 7-year offset between Be-10 in the four ice cores and the C-14 marker in the tree rings (and the ice cores lead the tree rings). Based on this discrepancy, the authors argue that the tree-ring sequence is correct and the ice-core age model is too old. Although I would not make the argument myself, I know some researchers might suggest that the tree-ring dates are too young (perhaps due to unrecognized missing rings) and the original ice core dates are correct. I would encourage the authors to explain more directly why this alternative explanation is not correct.

Since discovery of the $\Delta^{14}C$ excursion in 774/775 C.E. in 2012, an increasing number of tree-ring measurements have become available from various locations. These include sites at the upper tree line and northern tree line, including locations where there is a risk of missing tree rings, but also, crucially, in sites where temperature is not the dominating factor for ring width growth (e.g. German oaks), and hence not at risk of temperature-induced missing rings on any widespread scale. To date, no single tree-ring record has been measured for $\Delta^{14}C$ at annual resolution without registering the distinct radiocarbon excursion in 774/775 C.E. The coherence of a strong and distinct growth anomaly in 536 CE in virtually all tree-ring reconstructions across the Northern Hemisphere (NH) further supports our conclusion that none of the individual tree-ring reconstructions are subject to missing rings.

Of the four ice cores for which we showed ^{10}Be measurements, two previously were directly synchronized to GICC05 and do not provide any independent evidence supporting an older age for the 775 event. Potential causes for an age offset for the WDC06A-7 and GICC05 timescales are outlined above. Overall, the combined evidence from all ice-core data (annual-layer dating, the ^{10}Be excursion in 993, tephra findings in 536 and 946) supports the high accuracy of the new timescale and rejection of the hypothesis of a chronological bias in tree-ring chronologies.

Specific comments

In the Introduction, the authors make the point that major volcanic eruptions (as estimated from ice cores) are not always followed by short-term cooling (as inferred from tree rings) and that this lack of association may be caused by chronological error in one or both proxies. I agree with that point, but I wonder why Baillie (2008) is the sole source used to support that statement. Given the vigorous discussion of Mann et al's 2012 Nature Geoscience article on exactly that issue, I'd suggest adding a citation to that article and others written in response to emphasize more clearly that this apparent discrepancy is an important issue to resolve.

We focused in the introduction on the data/data mismatch prior to the past 1,000 years where the dating bias in existing ice-core chronologies is clearly the largest contributor to inconsistencies

between volcanic eruption dates and ensuing tree-ring growth impacts (a point stressed by [*Baillie*, 2008] and hence our citation of his work in the Introduction). In the revised manuscript, however, we have also summarized the ongoing discussion of the model/data mismatch for volcanic cooling response during the past 800 years and added additional citations [*Anchukaitis et al.*, 2012; *Esper et al.*, 2013; *Mann et al.*, 2012; *Mann et al.*, 2013].

Line 48: The point here (that efforts to link forcings to reconstructed climate require precisely-dated ice core and tree ring records) is perhaps a bit too narrow. Tree rings are only one type of proxy archive, and I can imagine the same statement would apply to lake sediments, speleothems, or really any other proxy. This section of the text may need to be reorganized to first emphasize the importance of chronological accuracy to these type of assessments, and then subsequently explain the particular relevance of proxy reconstructions from tree rings specifically.

Done.

51: "derived from" instead of "composed of". Also, time scales may be different but they cannot be unsynchronized, so the wording of this section needs to be changed.

Done.

55: What is the citation to support the statement about Pinatubo? Is that based on the current study?

We have added a citation to [*Douglass and Knox*, 2005] who used instrumental temperature data.

62: The phrasing of this sentence needs to be adjusted. As written, it implies that both C-14 anomalies have been identified in tree-ring records from all three regions, which is not correct. Based on the sources cited here, the 994 CE event has so far only been reported from tree-ring records in Japan. It would be helpful to revise this statement to provide a more accurate description of what anomalies have been reported where (and it would likely be appropriate to use more specific geographic terms; countries or regions instead of continents).

Done.

71: Again, this statement could be misinterpreted as saying that the C-14 anomaly has been found all tree-ring records containing rings spanning 774/775 CE. This sentence needs to be re-written so that readers understand that high-resolution C-14 analysis has only been conducted on a small handful of records, but that the consistency of this isotopic marker implies that these and other tree-ring records are correctly dated over (at least) the last 1200 years. Also, the phrase "established cross-dating procedures" is uninformative and could come across as defensive, so a citation and a reference to pattern-matching would be helpful.

Done.

84: By what evidence or argument is the 1257 Salamas eruption "well established"?

We removed the statement “well established” and included a citation instead.

110: It is not clear to me how the new volcanic forcing record provides a perspective on major historical events, or why the statement about European history connects to the other parts of the paper. To be honest, this comes across as unnecessary self-citation, and I don't see any reason to keep it.

Most previous volcanic forcing reconstructions do not extend before 500 AD and researchers were thus not able to adequately examine the possible contribution of major volcanic eruptions to many sudden climate variations (apparent in many climate proxies) and that coincided with known periods of major societal stress and change. Our newly revised volcanic chronology thus stands to clarify the role of major volcanism in many episodes of historical societal stress and change. To highlight this, we focus upon what is perhaps the most famous episode of major societal stress and change in the first millennium AD. This concerns the famous "536 event" and the ensuing climatic deterioration up to c.550, which has long been of contested cause, and is observed in a wide variety of climate proxies in the Northern Hemisphere. Our new volcanic time-series now clarifies the likely role of volcanism in identifying a sequence of major volcanic eruption beginning in 536, with further events in the 540s. We discuss this matter in more detail later in the paper. Our ultimate intent is to make a general statement: that human activities and volcanic history are intertwined, and that the new forcing reconstruction will allow a considerably improved exploration of these connections in the future.

120: The authors make the point that the 426 BCE and 44 BCE eruptions have previously not been regarded as large eruptions, but it's not clear what aspects of their results lead them to a (substantially) different conclusion. Given that they argue these events are among the very largest eruptions in the last 2500 years, it would be appropriate to explain more directly exactly what evidence supports that claim.

Large sulfate signals in Greenland ice-cores can originate from large and remote eruptions (e.g., Tambora 1815) or relatively moderate eruptions from nearby sources (e.g., Laki 1783, Iceland). For the latter, the climate effects are arguably smaller, and reconstructions of volcanic forcing usually correct for this effect using different scaling factors depending on the assumed (or known) source of the eruption [*Gao et al.*, 2008]. We propose that the 426 and 44 BCE eruptions were likely of tropical origin and caused among the largest radiative perturbations during the past 2,500 years because ice cores from Greenland and Antarctica contain exceptionally high volcanic sulfate concentrations at the same time (within their respective uncertainties), and were both followed by exceptional strong (and persistent) growth reduction in tree-ring records [*Salzer and Hughes*, 2007], as per Figure 2. Such responses are typically observed for large tropical eruptions during the Common Era (Figure 4).

Previously, a credible attribution was hampered by 1) the absence of a comparable complete sulfate record from Greenland [*Taylor et al.*, 1997]; 2) large dating uncertainties for ice core records in Antarctica relative to Greenland; 3) the apparent age offset of tree-ring indicated cooling extremes relative to ice-core derived volcanic forcing estimates [*Baillie and McAneney*, 2015]. We extended our statement with the above information.

123: The explanation of the tree-ring data used in this study needs to be revised to be more consistent and explicit about the data and the reasons for their selection. Throughout the article and the supplementary material, these data are described as tree-ring records, tree-ring based temperature reconstructions, and tree-ring networks. These terms are not interchangeable and their usage makes it more difficult to understand exactly what evidence is presented.

We have provided a more consistent terminology in our revised manuscript and more details below.

To my reading, the authors have assembled a set of extremely long (multi-centennial) tree-ring chronologies from five locations in the Northern Hemisphere. I would guess that these records were selected because (1) they span at least the last 1,500 years and (2) they primarily track local temperatures during the growing season (or summer season). First, it would be helpful if the authors

could explicitly provide the criteria they used to choose these records (and exclude others). Are there no other tree-ring records from the Northern Hemisphere that could be included in this assessment? There very well may not be any other records that fit the bill, but the authors needs to explain why these particular five records were used, and others were not.

Also, the authors combine the set of five tree-ring based temperature reconstructions (by averaging) and describe that average as an index of Northern Hemisphere temperature. I don't think it's reasonable to present that index as a hemispheric temperature reconstruction, given that the paper does not describe how well (or poorly) that average matches that specific climate variable. Developing a new hemispheric temperature reconstruction spanning the last 2,500 years would itself be a major effort, and simply averaging together a few select records (only 2 prior to 500 CE) does not convince me that these records provide a robust estimate of past temperature change across the hemisphere. To my mind, the authors need to acknowledge the limitations of making inferences about hemispheric temperature based on such a small number of proxy records. These records are clearly very important and rare, but the current manuscript is much too casual in presenting them as a hemispheric temperature record. I think this weakness could be addressed if the authors would describe these records as what they are: exceptionally long records of tree growth at locations where temperature is the main limiting factor. But these data describe tree growth; they are not a hemispheric temperature reconstruction.

In fairness, the paragraph starting on Line 123 does describe these records as estimates of tree growth, and my criticism is mainly aimed at the way they are described in the figure captions and the supplementary material.

There is, unfortunately, no continental-scale temperature reconstruction available covering the full 2,500 year span of our volcanic reconstruction to investigate the volcanic cooling impact over large spatial scales. We therefore assembled long and temperature-sensitive tree-ring chronologies for our analysis. We have now revised the manuscript by clarifying our methods and rationale as outlined below:

1) We selected from available databases and other accessible sources all annually-resolved proxy records from the Northern Hemisphere meeting the following three criteria: (1) >1,500 years long; (2) no assumed chronological uncertainty; (3) strong relationship to local temperature and/or already demonstrated sensitivity to volcanic forcing. In total, six records met the criteria [*Briffa et al.*, 2008; *Büntgen et al.*, 2011; *Esper et al.*, 2012; *Grudd*, 2008; *Salzer et al.*, 2014]. We excluded the Avam-Taymir tree-ring-width record from N-Siberia [*Briffa et al.*, 2008] in order to give stronger weighting to the two maximum latewood tree-ring density records [*Esper et al.*, 2012; *Grudd*, 2008], which represent the preferred parameter for reconstructing annually resolved temperature variations [*Esper et al.*, 2014]. The bristlecone pine tree-ring chronology exhibits a strong century-scale positive trend from approximately 1850 to the late 20th century [*Salzer et al.*, 2014a]. Due to this trend, along with concerns about a potential divergence from local temperatures [*Salzer et al.*, 2014b], we used the time period 1000-1099 CE as a common baseline period for standardizing tree growth anomalies among the five remaining records thus building a tree growth composite record which we now call “N-Tree” (z-scores). This record is not a reconstruction of NH temperatures *per se*, as the level of spatial representation varies through time. By averaging growth anomalies over large regions, however, synchronous growth reductions in these regions of strongly temperature-limited tree growth is a good indicator of the volcanic influence on past temperatures. Correlations between “N-Tree” (N=5) and the average of the

three regional PAGES 2k temperature reconstructions ("Arctic," "Europe," and "Asia" (N>275)) [*PAGES-2k Consortium, 2013*] between 1800 and 2000 are very high ($R^2 = 0.78$). This suggests that much of the large-spatial-scale variation in Northern Hemispheric regional temperatures is also captured by our select tree-ring records. Crucially, at least three records in "N-Tree" cover the time period from 138 BCE to the present, allowing a qualitative assessment of the potential volcanic cooling impact prior to the Common Era (Figure 2).

2) In order to quantify the climate impact during the Common Era and investigate regional differences, we only used tree-ring based JJA temperature reconstructions with strong demonstrated relationships to instrumental temperature data between 1901 and 2000 and high predictive skill. For regions where these criteria were met by several reconstructions (e.g., Scandinavia), we limited the analysis to the most recently updated reconstruction [*Esper et al.*, 2014]. We retained three regional reconstructions from the Central Alps, Scandinavia, and Northern Siberia (Jamal) [*Briffa et al.*, 2013; *Büntgen et al.*, 2011; *Esper et al.*, 2014]. By using these three regional reconstructions and the published continental-scale PAGES-2k "Europe" reconstruction [*PAGES-2k Consortium, 2013*], we quantified the average response of summer temperature to volcanic forcing during the Common Era (Fig.4).

We provided the necessary clarification of selection criteria in the new *Methods* section, and added a regional temperature reconstruction as time series (Figure 3) as well as the average response as derived by the superimposed epoch analysis using three different temperature reconstructions (Figure 4). From the extended analysis (restricted to the Common Era), we derived an estimate of absolute average summer temperature cooling for different regions following volcanic eruptions with respect to eruption size and source location from which we derived a quantitative relation between climate response and volcanic forcing.

176: I don't understand the connection between these two ideas. Why might the dating adjustment applied to ice-core records cause problems with multi-proxy reconstructions of temperature? Is it because ice cores are one of the proxy archives used to produce those reconstructions? Please clarify.

The dating adjustment proposed here will improve future multi-proxy reconstructions of temperature, because ice cores temperature proxies (i.e., $\delta^{18}O$ measurements) are widely used as an input parameter in multi-proxy reconstructions [*Hanhijarvi et al.*, 2013; *Mann et al.*, 2008]. The relative contribution of ice cores for example in continental-scale reconstructions for the Arctic and Antarctic regions is between 25 and 100 % during earlier time periods of the Common Era [*PAGES-2k Consortium, 2013*]. We clarified our statement accordingly.

Referee #2 (Remarks to the Author):

This is a landmark study. It integrates a remarkable variety of analyses into a major synthesis with important implications for climate science specialties, and with something of interest across a broad swath of the paleoclimate and climate modeling communities. Among the highlights is the discovery of abrupt shifts in the 10Be content of ice cores that enable the direct synchronization with tree rings. This analysis enables the authors to discern tropical from Northern Hemisphere eruptions, and therefore is the most thorough study to identify the climate-altering role of non-tropical eruptions, a significant contribution in itself. The study includes a major compilation of information on historical eruptions and new valuable geochemical analyses of tephras from Greenland ice. These are just some of the contributions of this top-notch study. I strongly recommend publication in Nature.

A relatively minor concern relates to the development of the tree-ring temperature reconstruction. Many studies have attempted to reconstruct Northern Hemisphere temperatures, so making up a new reconstruction on the fly seems a bit bold, although in the end, I don't have a better idea. Perhaps some additional explanation behind the approach would help lay some of the groundwork. Why did the authors choose the five tree-ring reconstructions that they did? Are they the only records from anywhere that extend at least 2000 years? Are they entirely independent of one another? How representative is the combined reconstruction target area of the entire Northern Hemisphere overall (or just land area of the NH)? Maybe the tree-ring reconstruction should be referred to as something like, "selected tree-ring composite".

Please see the response above to Reviewer 1's comments on the tree-ring reconstruction.

Related to this, the determination of the temperature associated with the volcanic cooling is somewhat difficult to understand. It would help to explain why the reconstruction was transformed to z-score units (same as standard deviations?) rather than C. And what was the rationale for standardizing to 1000-1099 CE? I suggest providing an estimate of how the z-score values relate to Northern Hemisphere temperature. There seems to be a miss-match between the volcanic-induced cooling quantified by the IPCC-AR5 (Fig. 5.8), which shows a temperature shift of < 0.2C for the 12 major eruptions since 1400 CE, compared with the estimate from the equation in the supplement note 11 (z-score = 0.34 X average temperature - 0.44). If I understand this correctly, the volcanic cooling of -1 SD calculated by this study represents about 2C, which is 10 times the value estimated by the IPCC. The IPCC included smaller eruptions and their temperature is for the average NH rather than Arctic/Europe focused, but the difference seems extreme and deserves attention. Perhaps the relation between the z-scores and some actual temperature could be derived more securely, along with an estimate of the uncertainty in the transformation (at least an r2 value for the regression used for the equation cited in note 11). Alternatively, it might be cleaner to use the average of the two PAGES 2k reconstructions that extend back 2000 years, as was done for Table S4, while recognizing that the temperatures are a slight underestimate of the cooling for the first millennium because the reconstructions include ice cores that missed the volcanic targets.

We improved and better clarified our methods to analyze the temperature response in the revised manuscript. The rational for standardizing over a time period outside the 20th century is given in our response to Reviewer 1, above. 1000-1099 was chosen in particular because no major growth anomalies were recorded in the individual tree-ring series that would skew the distribution of the values. In the revised manuscript, we use the tree-growth composite record in a more qualitative way to describe the relation of tree growth relative to forcing during the past 2,500 years, while we infer quantitative estimates of the cooling response from a subset of published regional-to-continental scale temperature reconstructions. The 5-year averaged summer cooling response calculated for all 24 major eruptions during the Common Era over three geographic regions (Alps, Scandinavia, and N-Siberia) was between 0.5 to 0.7°C. These values are in good agreement with the IPCC estimates for major eruptions over the past 600 years. The earlier mismatch noticed by the reviewer was the result of a typo in the formula (z-score = 0.34 x average temperature - 0.44), for which independent and dependent variables were accidently flipped. The correct formula should have been (average temperature = 0.34 x z-score - 0.44). We thank the reviewer for calling attention to this.

Regardless of the absolute temperature shift, the lingering cooling effect of the eruptions shown by the superposed epoch analysis is unexpected. Figure 2b and several panels in Figure 4 show that the cooling effect of volcanic eruptions persists after 10 years. This too contrasts with the IPCC's analysis (Fig. 5.8), which shows that temperatures mostly recover within 10 years. It would be useful to extend

the timescale (x-axis) in Figure 4 beyond 10 years following the eruptions to show the recovery time. Also, it's not clear what the "95% confidence intervals" represent in this figure. Is it the 2-sigma range of the temperature anomalies associated with the multiple eruptions?

We extended the time axis for the superposed epoch analysis to 15 years to better show the duration of growth reduction/cooling. To address potential causes/regional differences of the observed persistence of the volcanic climatic impact, we added panels to the superimposed epoch analysis in Figure 4. The 95% confidence intervals represented in Figure 4 is two times the standard error of the mean (2 s.e.m.) temperature anomaly associated with the multiple eruptions, which we specify in the revised manuscript.

A couple of minor points:

Lines 48-50. The statement that chronologies must be correct to within 1 year in order to attribute forcing to climate response is correct for volcanic eruptions, but is not correct for other types of forcing, including solar and orbital. Specify "volcanic forcing".

Done.

Line 64. The word "respectively" doesn't apply. There are two anomalies but three regions. Which of the anomalies was identified in which of the regions?

We clarified the sentence.

Line 170. Change "pandemics; as well" to "pandemics, as well"

Done.

Line 225. Omit the word "respectively".

Done.

Line 245. Omit the word "respectively".

Done.

Referee #3 (Remarks to the Author):

(A)

Sigl et al. propose a new interpretation of the volcanic forcing over the last 2,500 years, based on the comparison of several volcanic sulfate ice core records, from Greenland and Antarctica, and tree rings records that provides information on past temperature variations. They explained and solved the discrepancy between the volcanic records in ice cores and the answer in terms of cooling detected in tree rings records during the first millenium CE. The problem originated from the ice cores chronologies that were ca. 10 years too young compared with tree rings records.

The improvement of the chronologies is based (1) on a method for counting annual layers in the NEEM (Greenland) and in the WAIS Divide (Antarctica) ice cores, (2) on the detection of volcanic

sulfate peaks, (3) on the increase in beryllium-10 (10Be) concentration measured in the ice and related to two Solar Particles Events (SPE) that occured in 774-775A.D. and in 993-994 A.D., first detected in 14C tree rings records (Miyake et al., 2013, 2012).

(B) and (C)

The paper presents data of a high quality and a huge amount of information have been nicely interpretated. The results are well presented and the paper is easy to follow.

This work is of a high interest for the community studying natural climatic forcings, particularly, the influence of volcanic eruptions on climate and populations. This work will also be of importance for glaciology because it improves chronologies over the last 2,500 years and opens new perspectives for the interpretation of many other proxies.

The 10Be ice core data at the time of the 775 A.D. and the 994A.D. events are also expected by the community working on cosmogenic nuclides as well as the one studying the Sun. These two events have been first evidenced from 14C tree rings records and no 10Be ice core records were available until the paper of (Miyake et al., in press) who detected the 775A.D. event in the Dome Fuji ice core (Antarctica), and now, this work provides four new ice cores records, two from Greenland and two from Antarctica with a resolution never reached before and better than Dome Fuji.

All these new data have to be published and diffused largely.

(D), (E) and (F)

However, I have three main remarks related to the 10Be records.

(1) The NEEM 2011-S1 ice core has the most constrained chronology, it is based on annual counting layers, on 5 volcanic events and on the 775A.D. event found in the 10Be record.

10Be measurements are not continuous and have been made only around the age of 775A.D. We can see from the table provided in the supplementary material that 21 measurements have been made before and after the age of 775A.D. determined in the previous agescale (so from 752 to 795 A.D.). Finally, the 775A.D. event was found in 768A.D. on the NEEM-2011-S1 old age scale, 7 years before the 14C tree rings records. This difference was taken into account to establish the new chronology and to test it, the second event, in 994 A.D., was used to check if it was improved. They are only 26 10Be analysis for the 994A.D. event, in addition, measurements stopped in 995.5 AD. on the old age scale, which means that the authors hypothesized a systematic 7 years lags between the age scales for this record but also for all the other ice core records.

The 775A.D. has been well identified in the NEEM-2011-S1, NGRIP and WDC ice cores, we can see the corresponding 10Be concentration peaks but it would have been useful to show more 10Be data before the 775A.D. event in the WDC (only 6 measurements before the peak) and NGRIP (only 2 measurements before the peak) ice cores.

Figure 1 illustrates that the ice core records of WDC and NGRIP were sampled in order to test existing timescales and/or to investigate ^{10}Be deposition relating to the 775 SPE, (for some records the location of the peaks in relation to sampled depth range indicates that we almost missed the peak due to the unknown time scale error). By contrast, the NEEM-2011-S1 ice core was sampled specifically

to test an alternative dating scenario, and we thus sought to analyze more samples to estimate background ^{10}Be concentrations prior to the 775 event. We agree with the reviewer that more samples especially before 775 SPE would be helpful to better estimate background concentrations of ^{10}Be, but this was not the aim of this study. A companion paper (will be submitted directly after publication of this study) discusses these topics in more detail. Irrespective of these issues, the ^{10}Be peaks for NEEM-2011-S1, NGRIP and WDC are outside the range of the typical inter-annual ^{10}Be concentration variability (calculated from annual values), and no secondary excursion of similar magnitude is expected taking into account all ^{14}C and ^{10}Be measurements performed to date at quasi-annual- [*Miyake et al.*, 2015] to-decadal resolution for both hemispheres [*Usoskin et al.*, 2013].

I am wondering if it would not be better to put the TUNU2013 10Be record in the supplementary material because how can the authors be sure that they identified the 775A.D. event in this record? There are only 9 measurements going from 762.7 to 770.3 A.D. on the original NEEM-2011-S1 chronology. The amplitude of the 10Be increase is not discussed because the value of the background level cannot be determined with a 8-yrs record. On short timescales, the production of cosmogenic nuclides (14C, 10Be,..) is modulated by the 11-yr solar cycle and by solar activity (quiet vs. active phases). Recently, Güttler et al. (2015) took into account the 11-yr modulation to discuss the amplitude of the 775A.D. event found in the 14C tree rings record.

We respectfully disagree, given that the relative age uncertainty for the TUNU2013 ice core with respect to the NEEM-2011-S1 ice core (to which the TUNU2013 ice core is synchronized) does not exceed ±1 year at this depth. Our strong confidence in the synchronization of TUNU2013 comes further from a very distinct match in selected volcanic trace element profiles in 752–764 (NS1-2011 dating). We are, therefore, confident that the enhanced ^{10}Be values of >30 x 10^3 atoms g^{-1} for two years present the signature caused by SPE in 775 (it exceeds the expected solar-modulated ^{10}Be variability). Duration and the absolute concentration values measured at TUNU2013 are almost identical to the NEEM-2011-S1 core, as would be expected for an ice core drilled at the same latitude, at comparable elevation, and where aerosol deposition in winter/spring is dominated by wet rather than dry deposition processes [*Hutterli et al.*, 2007]. To address the reviewer's concern, we have added our estimates for the relative synchronization uncertainties of TUNU 2013 around 775 CE to the method section as well as to the Figure 1 caption.

It is expected that the 10Be concentration in ice cores varies according to this 11-yr cycle, so to determine the background level, the 10Be record should at least cover 22 yrs corresponding to two solar cycles. In addition, there is no annual resolution (no seasonal or annual chemical signature) at this site (end of the section 10 of the supplementary material) which means there is also an uncertainty on the agescale that is higher than that of NEEM-2011-S1 or WDC-2014.

We agree that without prior synchronization, ideally two cycles should be determined to estimate background concentrations (which we did for WDC and NEEM-2011-S1). The TUNU2013 high-resolution chemistry measurements are sub-annually resolved, and annual cycles can be identified in many chemical species. However, given the low accumulation rates of 10 cm ice $year^{-1}$, the interpretation becomes more ambiguous than for higher accumulation sites (e.g., NEEM-2011-S1, NEEM) which is why the TUNU2013 record has been synchronized to the NEEM-2011-S1 ice core record. We clarified our statement in the methods section to emphasize this point.

Why is the TUNU2013 sulfate record not shown?

The TUNU2013 sulfur record has not been shown in Figure 2 primarily to keep this already complex figure clear and readable. The general trends in TUNU2013 are very similar to that of NEEM-2011-S1. We did show, however, the TUNU sulfur record in Extended Data Fig. 4 focusing on 6th to 7th century volcanic records, which we have now moved in the revised manuscript to Figure 5 in the main text.

(2) Reconstruction of temperature anomalies taking into account both volcanic and solar forcings are represented in the figure 4. Maybe I missed the information, but the authors do not really explained how they proceeded to take into account the periods of low or high solar activity. There is one sentence in the paper (lines 143 to 145) mentioning the work of (Steinhilber et al., 2012) and some indication on the Total Solar Irradiance are given in the figure caption despite the missing references (please add the references). Some information and explanation should be added in the supplementary material.

What I understand is that the authors used the TSI reconstruction proposed by Steinhilber et al. (2012) to determine the periods of low or high solar activity. In the figure caption, periods of low solar activity correspond to TSI < 1st quartile (please, some explanation is needed here) during which 6 large volcanic eruptions occurred and periods of high solar activity correspond to TSI > 3rd quartile during which 7 eruptions were observed. I suppose that the remaining 15 large volcanic eruptions, on a total of 28, occurred during periods of TSI going from the 1st to the 3rd quartile.

It would be interesting to investigate the temperature anomaly during period of moderated TSI values in order to check if 'the magnitude of the cooling following large eruptions 'is' relatively insensitive to solar activity' (line 145).

In the revised manuscript, we removed the previous analysis because: (1) the number of volcanic events during periods of both high and low solar activity is relatively small, resulting in large uncertainties in the results; (2) the previously used methodology of superimposed epoch analyses is arguably not the best tool to attribute solar and volcanic influence on past temperatures given the variability of solar activity on decadal to multi-decadal timescales. Removing the statement here also allowed us additional space needed to extend our treatment of volcanic impacts on temperatures in response to reviewer comments.

(3) The term '10Be' anomaly is often used in the paper to refer to the 775A.D. and the 994A.D. events (e.g. lines 68 and 70). The origin of these events is still under debate but it should be a SPE (e.g. (Güttler et al., 2015; Miyake et al., in press; Usoskin et al., 2013)). It means that high energetic particles will induce an increase in the cosmogenic nuclides production and as a result an increase in the 10Be concentration in the ice so there is no anomaly in the process. The word 'anomaly' is not used in all the publications mentioning the 775A.D. event, it would be better to use another term.

We revised the manuscript to consistently use the terms “rapid increase of ^{10}Be concentration in ice cores” and “rapid increase in the ^{14}C content in tree rings.” or refer to the events as “775 event” and “994 event”.

There are also a few minor comments:

- lines 72 and 73: the annual resolution is possible only on the WDC, NEEM and NGRIP sites because of the high accumulation and the annual layers detected with chemical compounds (e.g. sea salts) but the accumulation rate at TUNU and B40 do not allow to reach an annual resolution, it is rather a high resolution.

The ^{10}Be measurements of TUNU2013 were performed at quasi-annual resolution, meaning that on average one ^{10}Be sample included one year (and assuming constant snowfall rates), but without sampling at the respective annual layer boundaries. We corrected our statement to “approximately annual resolution” in the main text and provide specific information in the method section.

- line 89: would it be possible to give an explanation on 'the three post-volcanic atmospheric anomalies' ?

The three post-volcanic atmospheric anomalies are well-dated historical observations of atmospheric phenomena with known association to explosive volcanism (e.g., diminished sunlight, discolored solar disk). Two examples are given in Figure 5. A more detailed summary is given in Extended Data Table 3, and an extensive list is provided as Supplementary Data. The observed atmospheric dimming effects are caused by high concentrations of volcanic ash and/or sulfate aerosol particles present in the atmosphere that scatter incoming solar radiation. What is anomalous for these three events is the long duration of the “volcanic dust veil” lasting for up to one year, suggesting significant atmospheric aerosol loading.

- lines 143 to 145: as mentioned in the main comments, more information are needed here.

Done.

- figure 1: is the figure 1a useful here ? On the graph c, the delay between NEEM and the 14C record is 7 yrs, not 6 yrs (7 yrs is the value given in the paper).

Figure 1a is a simplified summary of the inconsistency in tree-ring and ice-core chronologies using previous chronologies which were the starting point of the analyses performed here. We checked the ^{14}C data and subsequently corrected the figure. Seven years is the correct offset for the 994 CE event.

(G) References

- line 31: the papers of Miyake et al. (2012, 2013) are mentioned but those of Usoskin et al. (2013) (ref. 17) or Jull et al. (2014) (ref. 16) can be added here. The paper of Güttler et al. (2015) can also be added.

Done.

- line 47: 'including solar (e.g. 10Be)...activity', maybe some references should be added here. Some TSI reconstructions have been proposed, the authors can cite a few ones such as (Bard et al., 2000; Delaygue and Bard, 2011; Steinhilber et al., 2012, 2009; Vonmoos et al., 2006) but there are many other publications. Another possibility is to cite a review that had been done by Usoskin because all these publications are cited inside (Usoskin, 2013).

We removed the analysis of possible solar influences, and extended the quantification of temperature response to volcanic forcing.

- line 62: two new references can be added (Miyake et al., in press, GRL) and (Güttler et al., 2015).

Done.

- line 66: why is the paper on Steinhilber et al. (2012) cited here? If the authors want to mention the response of cosmogenic nuclides production to SPE, they would rather cite all the references of the

line 62, if they want to describe the general process of cosmogenic production , they should cite older papers, for example (Kovaltsov and Usoskin, 2010; Masarik and Beer, 2009; Webber et al., 2007)...

We added more appropriate references when discussing the general process of cosmogenic production.

- line 78: one sentence can be added for the comparison with the Dome Fuji 10Be results (Miyake et al., in press).

Done.

- lines 121 and 123: it seems that references related to tree-rings are missing.

Done.

- figure captions : it seems that all the references related to 14C and tree rings have been forgotten.

Added as suggested.

- supplementary material ref 18: 'Heikkila' instead of 'Heikkilae'

Done.

(H) Clarity and context

The paper is clear and well written (abstract, introduction and conclusion) and easy to read.

All the information and tables provided in the supplementary material are useful and relevant.

Please note that all referees made recommendations related to additional references. We responded to all of these suggestions, thereby strengthening the manuscript, and thank the referees for their attention to this improved scholarship.

References:

Anchukaitis, K. J., et al. (2012), Tree rings and volcanic cooling, *Nat Geosci*, ***5***(12), 836-837.

Baillie, M. G. L. (2008), Proposed re-dating of the European ice core chronology by seven years prior to the 7th century AD, *Geophys Res Lett*, ***35***(15) L15813.

Baillie, M. G. L., and J. McAneney (2015), Tree ring effects and ice core acidities clarify the volcanic record of the 1st millennium, *Clim. Past*, ***11***, 105-114.

Briffa, K. R., T. M. Melvin, T. J. Osborn, R. M. Hantemirov, A. V. Kirdyanov, V. S. Mazepa, S. G. Shiyatov, and J. Esper (2013), Reassessing the evidence for tree-growth and inferred temperature change during the Common Era in Yamalia, northwest Siberia, *Quaternary Sci Rev*, ***72***, 83-107.

Briffa, K. R., V. V. Shishov, T. M. Melvin, E. A. Vaganov, H. Grudd, R. M. Hantemirov, M. Eronen, and M. M. Naurzbaev (2008), Trends in recent temperature and radial tree growth spanning 2000 years across northwest Eurasia, *Philos T R Soc B*, ***363***(1501), 2271-2284.

Büntgen, U., et al. (2011), 2500 Years of European Climate Variability and Human Susceptibility, *Science*, ***331***(6017), 578-582.

PAGES-2k Consortium (2013), Continental-scale temperature variability during the past two millennia, *Nat Geosci*, ***6***(6), 339–346.

Douglass, D. H., and R. S. Knox (2005), Climate forcing by the volcanic eruption of Mount Pinatubo, *Geophys Res Lett*, ***32***(5), L05710.

Esper, J., U. Buntgen, J. Luterbacher, and P. J. Krusic (2013), Testing the hypothesis of post-volcanic missing rings in temperature sensitive dendrochronological data, *Dendrochronologia*, ***31***(3), 216-222.

Esper, J., E. Duthorn, P. J. Krusic, M. Timonen, and U. Buntgen (2014), Northern European summer temperature variations over the Common Era from integrated tree-ring density records, *J Quaternary Sci*, ***29***(5), 487-494.

Esper, J., et al. (2012), Orbital forcing of tree-ring data, *Nat Clim Change*, ***2***(12), 862-866.

Gao, C. C., A. Robock, and C. Ammann (2008), Volcanic forcing of climate over the past 1500 years: An improved ice core-based index for climate models, *J Geophys Res-Atmos*, ***113***(D23).

Grudd, H. (2008), Tornetrask tree-ring width and density AD 500-2004: a test of climatic sensitivity and a new 1500-year reconstruction of north Fennoscandian summers, *Clim Dynam*, ***31***(7-8), 843-857.

Hanhijarvi, S., M. P. Tingley, and A. Korhola (2013), Pairwise comparisons to reconstruct mean temperature in the Arctic Atlantic Region over the last 2,000 years, *Clim Dynam*, ***41***(7-8), 2039-2060.

Hutterli, M. A., T. Crueger, H. Fischer, K. K. Andersen, C. C. Raible, T. F. Stocker, M. L. Siggaard-Andersen, J. R. McConnell, R. C. Bales, and J. F. Burkhart (2007), The influence of regional circulation patterns on wet and dry mineral dust and sea salt deposition over Greenland, *Clim Dynam*, ***28***(6), 635-647.

Mann, M. E., J. D. Fuentes, and S. Rutherford (2012), Underestimation of volcanic cooling in tree-ring-based reconstructions of hemispheric temperatures, *Nat Geosci*, ***5***(3), 202-205.

Mann, M. E., S. Rutherford, A. Schurer, S. F. B. Tett, and J. D. Fuentes (2013), Discrepancies between the modeled and proxy-reconstructed response to volcanic forcing over the past millennium: Implications and possible mechanisms, *J Geophys Res-Atmos*, ***118***(14), 7617-7627.

Mann, M. E., Z. H. Zhang, M. K. Hughes, R. S. Bradley, S. K. Miller, S. Rutherford, and F. B. Ni (2008), Proxy-based reconstructions of hemispheric and global surface temperature variations over the past two millennia, *P Natl Acad Sci USA*, ***105***(36), 13252-13257.

Miyake, F., A. Suzuki, K. Masuda, K. Horiuchi, H. Motoyama, H. Matsuzaki, Y. Motizuki, K. Takahashi, and Y. Nakai (2015), Cosmic ray event of AD 774-775 shown in quasi-annual 10 Be data from the Antarctic Dome Fuji ice core, *Geophys. Res. Lett., in press*, doi:10.1002/2014GL062218.

Salzer, M. W., A. G. Bunn, N. E. Graham, and M. K. Hughes (2014a), Five millennia of paleotemperature from tree-rings in the Great Basin, USA, *Clim Dynam*, ***42***(5-6), 1517-1526.

Salzer MW, Larson ER, Bunn AG, Hughes MK (2014b). Changing climate response in near-treeline bristlecone pine with elevation and aspect. *Environmental Research Letters*, **9**: 114007 doi:10.1088/1748-9326/9/11/114007.

Taylor, K. C., R. B. Alley, G. W. Lamorey, and P. Mayewski (1997), Electrical measurements on the Greenland Ice Sheet Project 2 core, *J Geophys Res-Oceans*, ***102***(C12), 26511-26517.

Usoskin, I. G., B. Kromer, F. Ludlow, J. Beer, M. Friedrich, G. A. Kovaltsov, S. K. Solanki, and L. Wacker (2013), The AD775 cosmic event revisited: the Sun is to blame, *Astron Astrophys*, ***552***, *L3*.